LA-UR -87-2881

CONF-8705193--2

Los Alamos National Laboratory is operated by the University of California for the United States Department of Energy under contract W-7405-ENG-36

TITLE: DIMENSIONAL ANALYSIS OF NONLINEAR OSCILLATIONS IN BRAIN, HEART AND MUSCLE

LA-UR--87-2881

DE87 014749

AUTHOR(S): G. Mayer-Kress
F. Eugene Yates
Laurel Benton
M. Keidel
W. Tirsch
S.J. Poppl
K. Geist

SUBMITTED TO: Proceedings for the 7th Annual Conference "Nonlinearity in Biology & Medicine"

DISCLAIMER

Los Alamos National Laboratory
Los Alamos, New Mexico 87545

Dimensional Analysis of Nonlinear Oscillations in Brain, Heart and Muscle

G. Mayer-Kress [*,†,‡], F. Eugene Yates[†], Laurel Benton[†], M. Keidel[°], W. Tirsch[°], S.J. Pöppl[°], K. Geist[‡,◂]

Abstract We present some numerical studies on the dimensional analysis of temporal oscillations measured in the human electroencephalogram (EEG), heart rates (HR), and muscle tremor. We show that it is insufficient to characterize the individual system by a single dimension value alone. We give some detailed numerical analysis of the scaling structure of the attractors reconstructed from the time signal.

Our methods are based on the concept of local gauge functions which we derive from the raw signals as well as from the transformed signal obtained from singular value decomposition. We were able to confirm and improve earlier results on the change of dimensionality of EEG signals. For heart rates and muscle tremor we observe significant changes in the dimensionality depending on the state of the system.

We further try to indicate which factors enter dimension estimates and where specific problems lie in each of the examples.

* Laboratory for Biological Dynamics and Theoretical Medicine, Institute for Nonlinear Science, UCSD
† Crump Institute for Medical Engineering UCLA, 405 Hilgard Avenue, Los Angeles, CA 90024-1654
‡ Center for Nonlinear Studies, MS-B258, Los Alamos National Laboratory, Los Alamos, NM 87545
° Neurologische Klinik und Poliklinik der TU München, West-Germany
◂ 3. Physikalisches Institut der Universität Göttingen, West-Germany

1. Introduction

There are many mathematical models in the literature, which try to explain the origin of self generated rhythmical behavior in biological systems [1,2,3]. Some of the models are of a deterministic and nonlinear nature which can undergo a Hopf bifurcation to a periodically oscillating state. Pure periodicities are, however, rarely realized in biological systems and thus stochastic forces are introduced to reproduce the irregularities in the oscillations. The origins of these stochastic forces can be in the uncontrolable influences of microscopic processes, which perturbe the frequencies and phases of the oscillators.

Other sources of irregularities can be feedback loops which couple the oscillating system to other slowly varying processes in the organism. For instance in the generation of the EEG, as well as in other processes, which are generated by neural activity, one can envision that uncorrelated firings of neurons might cause quasi-stochastic perturbations. Here we are more interested in slow changes of the dynamics, e.g. changes in mental activity (shift of concentration, sensory input etc.). In the variability of heart rates it has been possible to identify several low frequency perturbations as discussed in more detail below. In the context of muscle tremor the main source of nonstationarity seems to be the tiring of the muscle.

In this paper we don't try to model the biological mechanisms which generate these oscillations but we try to describe and apply some methods from nonlinear dynamical systems theory which we have used to study the oscillatory signals from three of the most prominent biological oscillators: The electrical signal from human brains (EEG) and hearts (EKG) and muscles (EMG). During the last couple of years one could observe a growing research activity of analysing dynamical properties of biological systems both in classical terms [4] and using algorithms from nonlinear dynamical systems like fractal dimensions and entropies [5]. It appears that in the field of nonlinear dynamical analysis we are

still in the beginning stages of a methodological evolution. Thus there typically exists common agreement as of how to compute and interprete spectral information and also about possible artefacts that have to be taken care of. The situation is different, however, in the calculation of, say, fractal dimensions from a timeseries. Many different algorithms and methods have been proposed which efficiently produce converging results in simple cases ($d < 3$), but for more complicated sets the different methods seem to have problems in reproducing reliable dimension values with a realistic number of data points.

There have been some efforts, however, to standardize the methods of dimension calculation, so that results from different authors can be compared ("pecos standard").

2. Estimating the *dominant* dimension from local gauge functions

2.1 Geometrical reconstruction

In this section we would like to give a brief overvue of the concepts of dynamical dimension estimates and then describe in some detail the methods we have used to obtain an unbiased estimate of the most dominating dimension and some detailed structure of the scaling properties of the reconstructed attractors. We start with the -now classical- method of time-delayed variables for reconstructing attractors [6]: Assume we are measuring a single variable time-series $x(t_m) = x_m$ then we can reconstruct vectors $\vec{x}_m$ in a n-dimensional state space through time delay coordinates: $\vec{x}_m = (x_m, x_{m-k}, x_{m-2k}, \ldots, x_{m-(n-1)k})$, where m runs from $(n-1)k+1$ to the number n_{data} of data points and k is the time delay [6]. In fig. 1 we plot the time series x_m and also state space reconstructions in the plane ($n = 2$) for two different delay times $k = 1$ and $k = 4$.*

The time delay should be chosen in a way that the coordinates of $\vec{x}_m$ are maximally independent. We use the concept of mutual information content [7,8] to determine the optimal delay time.

* Here and in the following figures we want to illustrate our method on heart rate data from a healthy female, taken during regular daily activity with the help of a Holter monitor. A more detailed description follows below.

2.2 Local Gauge functions and pointwise dimensions

From the data vectors $\vec{x}_m$ we select a subset of n_{ref} equally spaced (in time) reference vectors $\vec{\xi}_j = \vec{x}_{j\nu}$ where $\nu = [\frac{n_{data}}{n_{ref}}]$. For each of the n-dimensional reference vectors we determine the local gauge function $N_{\vec{\xi}_j}(r) = \sum_{i=1}^{n_{data}} \Theta(r - \|\vec{x}_i - \vec{\xi}_j\|)$, which counts the number of data points in a neighborhood of size r[1]). In a log-log-representation this function typically exhibits a scaling region $[r_{min}, r_{max}]$ [2]) over which a slope can be defined. This slope is then interpreted as the pointwise dimension $d_{\vec{\xi}_j}$ of the system at point $\vec{\xi}_j$ (see e.g. [5,9,10]).

Due to the non-uniformity property [11] of generic attractors we expect that the location as well as the size of the scaling region depends on the reference point $\vec{\xi}_j$. In the widely used Grassberger-Procaccia algorithm [10] for dimension estimation the average value of $N_{\vec{\xi}_j}(r)$ is computed over all reference points $\vec{\xi}_j$ at a fixed value of r. This induces for the case of finite scaling regions an extra error which can be avoided by computing the pointwise dimension individually for each of the reference points In the strict sense the dimension is determined through the scaling behavior at infinitesimal distances. In a practical sense this is not only unfeasable but also in many cases unphysical: The relevant dynamics which we want to study is not necessarily the dynamics at very small scales, where we know that noise becomes dominant. Also for very small scales and limited data sets we know that the statistics becomes bad. Therefore we want to study the dominant dimension in the sense that it describes the scaling behavior with the least disturbances (i.e. the best fit of a straight line in a log-log plot) over the largest range [12]. In fig. 2 we show a series of gauge functions in a log-log representation for embedding dimensions $1 < n < 20$ for the same heart rate data as in fig.1. We see for small values of $\log r$ the effect of the finite resolution of the measurement ($\approx 1\%$). The solid line indicate the

[1]) $\Theta(r) = 1$ for $r > 0$ and $\Theta(r) = 0$ elsewhere

[2]) This means that for $r \in [r_{min}, r_{max}]$ we have $N_{\vec{\xi}_j}(r) = c(\vec{\xi}_j)\, r^{d_{\vec{\xi}_j}}$ where $c(\vec{\xi}_j)$ is a position dependent scale factor.

fit region for each embedding dimension determined by the algorithm. We think that this method corresponds in a more systematic way to the procedure of extracting a dimension value from a visual inspection of the dimension curves. In fig. 3 we can see an example of how the scaling range is selected by our algorithm for embedding dimensions $n < 20$.

In order to minimize the bias in dimension estimates we introduced an algorithm which determines fit-range, goodness of fit (GF) and estimated dimension automatically for each reference point and for each embedding dimension. In this way we want to make sure that the same criteria are entered in each of the data sets and therefore results become better reproducable and can be compared with other data sets. The main assumption in the "dominant" dimension estimate is that the relevant scales at each location on the attractor can be found by searching -for a given minimal scaling factor $\alpha = \frac{r_{max}}{r_{min}}$ over which the attractor scales- for that value of *log r* for which the fit of a linear segment of length *log* α to the log of the gauge function becomes optimal. In order to get well defined conditions and also in order to make optimal use of the local scaling properties, we expand the scaling region in the next step until the specified goodness of fit is reached. We use linear interpolation to compensate for the discontinuities due to the finite coarseness of our sequence of distance values r_k.

Since our reference points are sampled with equal time intervals $\nu = [\frac{n_{data}}{n_{ref}}]$ we obtain a sequence of dimension values which reflects the temporal ordering on the attractor. This temporal information is completely lost in a direct calculation of the Grassberger Procaccia (GP) dimension. Our method is also superior to repeated calculation of the GP- dimension on subsets of the time series, since in that case one is considerably more limited in the number of relevant data points available for the estimate.

It is possible through our method to localize specific regions on a reconstructed attractor which are responsible for significant changes in the apparent local dimensionality.

In our fitting procedure we determine a dimension estimate for each value of the embedding dimension. Again for stability reasons we want to avoid a discontinuous jump in the dimension estimate as a function of the embedding dimension throug a change in the fitting interval. Thus we monitor the dependence of the fitting interval, selected by our algorithm, on the embedding dimension and in most cases the discontinuity in the dimension values is due to this shift in the fit region. In fig.3 we show an example where we have plotted the extension of the fit region for increasing embedding dimensions for one specific reference point. In fig. 4 we plot the pointwise dimension obtained in this way as a function of the reference point. This is equivalent to probing the attractor at different geometrical locations and also at different instances in time. We think that this information is very helpfull in associating changes in the complexity of the dynamics with geometrical features of the reconstructed dataset and there for get some better insight into the characteristics of the system. The oscillating variation of the dimension values in fig. 4 is quite apparent, its clinical interpretation is not clear yet.

2.3 Singular value decomposition

If we chose a optimal delaytime for which the mutual information between x_m and x_{m-k} becomes minimal then we only know that the coordinates of the data-vectors $\vec{x}_m$ are pairwise optimally independent but still there might be a large redundancy contained in the datavectors through e.g. higher order correlations. A method which represents the data vectors in a basis with minimal correlation has been first applied to dimension calculations by Broomhead and King [14,15]. It is based on a singular value decomposition method which corresponds to an expansion of the datavectors into modes which are dominantly contained in the signal. In their original paper Broomhead and King were interested in the high frequency content of their signal and therefore used a high sampling rate and reconstructed vectors which would cover windows of the timeseries of a period corresponding to

the highest relevant frequency contained in the signal. Since most of the chaotic phenomena appear in the subharmonic low frequency range we have chosen windows (patterns) in the timeseries of maximal length of the order of typical decaytimes of correlations. To be more precise, we determined the window lenght as the product of the characteristic time determined by the first minimum of the mutual information content and the maximal embedding dimension used for the dimensional analysis without singular value decomposition (SVD). Thus the maximal time segment covered by any data vector is of the same order in both methods. We expect that patterns of a larger temporal extension would be too contaminated by noise which will be amplified by the chaotic dynamics of the system. In fig. 5 we show the gauge function of the same reference point as in fig. 2 after SVD with windowlength 100. In fig.6 we see that the oscillating structure of the time dependence of the pointwise dimension is also visible after SVD. In fig. 7 we show the histogram for the data of fig. 4 (solid lines) and for fig. 6 (dotted lines). Typically the distribution becomes more normal after SVD.

In fig. 8 we show the dependence of the estimated dimension value $< d_{\vec{\xi}_i} >_{\vec{\xi}_i}$ on the embedding dimension n. The error bars correspond to to the standard deviation of the dimension distribution over the reference points which have reached the minimal goodness of fit. They are solid lines for the original data and broken lines after singular value decomposition. Note the fast saturation to a smaller value in the latter case. This seems to be typical for this method, but we have cases where this can lead to underestimation of the true dimension values [16]. In order to get some idea of the overal scaling properties of the datasets we plot the percentage of reference points which reach a certain goodness of fit GF as a function of GF and embedding dimension n. We see in fig. 9 that without SVD most of the reference points fulfill our criterion for $GF > 0.3$ for our example set. The scaling properties become much better in the case of SVD, and it is also typically better for

data of brain- or muscle oscillations. We also tested how the observed dimension depends on GF and on the embedding dimension n. The results for our test example are presented in fig. 10. We observe a steady increase of the dimension when we increase GF and n. Again we see much better convergence after SVD (fig. 11). The opposite tendency seems to hold for the standard deviation of the dimension values, i.e. a good scaling behavior (small GF) is associated with a high variability of the dimension values (fig. 12). A more detailed information about this phenomenon can be obtained in fig. 13, where we show how the histogram of fig. 6 evolves with increasing embedding dimension n.

In the following we try to examine a few specific examples from the three areas brain, heart and muscle and discuss some problems and results.

3. Dimensionality of the Electroencephalogram (EEG)

There exists now a fairly large number of publications on estimating dimensions from EEGs [17,...,24].

It is known for a long time that the electrical signal of the EEG is in some way related to the mental activity of the brain. So, for instance it is possible for trained individuals to distinguish between sleep and awake states by visually inspecting the EEG. Thus there have many attempts to find some quantitative observables which could measure these changes [4]. A limited success was achieved by fourier analyzing the EEG signal and specifying the different mental states according to the distribution of the power of the signal in different frequency bands. The most famous among them is the frequency band around $10Hz$ (alpha waves) which is in some way related to a relaxed state with eyes closed. The implicit assumption in this and similar ways of analysis is that the "active modes" in the brain which produce the electro-magnetic signal, are linear periodic oscillators. It is known, however that the number of these fourier modes can be much larger than the number of

modes which actually are responsible for the physical, or in this case, bio-chemical processes [25].

Thus, while spectral methods, which analyze frequency bands are optimized for regular periodic or quasi-periodic signals, the applicability of these methods becomes very limited in cases where the signal is intrinsically very irregular without very sharp and well defined frequency bands. This situation of deterministic chaos is known to be fairly common in nonlinear dynamical systems and is discussed as an origin of many biological and clinical cases of temporal disorders.

Improvements in nonlinear methods should make it possible to classify EEg signals according to their degree of complexity or according to the number of nonlinear modes which are generating them.

3. Influence of the excitatory anestetics fluroxene

One important application of EEG analysis is anesthesia, where a reliable monitoring and control of its depth is still a problem which causes many fatalities every year. For a certain excitatory anestetic an increase in the observed Grassberger-Procaccia was reported [17,23,24]]. The dimension, measured at the lead P3-O1 was reported to increase from $d_G P = 4.3 \pm 2.2$ before anesthesia to a value of $d_G P = 8.0 \pm 3.8$ during medium fluroxene anesthesia. The computation of the averaged pointwise dimension yields in the first case a value of $d_{AP} = 6.4 \pm 1.2$ and in the second case a value of $d_{AP} = 7.1 \pm 0.5$ [24]. We redid the calculations with slightly modified algorithm (details in the way the optimal fit range is obtained and the omission of datapoints which are strongly correlated with the reference points) and found values of $d_{AP} = 5.2 \pm 1.3$ for $GF = 0.1$ ($d_{AP} = 6.7 \pm 2.0$ a for $GF = 0.2$) and $d_{AP} = 8.7 \pm 1.1$. In fig. 14 we see how, for a given embedding dimension, the observed dimension increases when the fit gets worse. In a stronger sense this is true

for the anesthesia data. For the dimensions obtained after singular value decomposition the same tendency holds but for $GF < 0.5$ we still have $d_{SV} < 5.0$.

These results show a delicate dependence on details especially at high values of the dimension. Also we see the estimate [26] confirmed that dimension values considerably above $d = log_{10}(n_{data})$ are difficult to reproduce. Finally we used the method of singular value decomposition (figs.15,16) on these data and found values of $d_{SV} = 4.7 \pm 1.3$ and $d_{SV} = 6.3 \pm 1.5$. The encouraging result is that we consistently find an increase in the dimensionality which supports the conjecture that it would be difficult in biological systems to estimate the absolute value of the dimension but it might be a valuable tool for detecting relative changes in the complexity of the dynamics.

4. Analysis of Variation in Heart Rate and of Heart Rate Variability

The human heart is a nonlinear, near-periodic oscillator (van der Pol) that operates on a "squirt-relax" two-process cycle producing an asymmetric waveform. Associated with the mechanical cycle is an electrical cycle of the same period but of more complex waveform. The heart rate is usually determined by counting the number of beats (maxima in the pressure cycles) per minute that result from the mechanical pumping of the heart into the blood vessels. But the heart rate can also be defined as the number of R waves (or P waves) in the electro- cardiographic signal of each mechanical cycle. Because the R waves are much larger than the P waves, the RR intervals (ranging from 300 *msec* for fast heart rates to 2,000 *msec* for slow heart rates in adults) are often used as the database. A ordered set suitable for "time series" analysis can then be created by plotting the RR interval magnitude (msecs) vs. interval number in the sequence of heart beats (of which there are approximately 100,000 per 24 hours) (see fig. 1). Standard power spectral density analysis can be applied to such a series. The shape of the power spectral density function

then gives some indication about variations in heart rate, both periodic and broad band noise.

For a closer analysis of the variability of heart rate, it is customary to examine the time series of RR(n+1) - RR(n) (hereafter designated DRR) where n is the beat number in the temporally ordered sequence. To correct for the fact that many natural processes have constant coefficients of variation (i.e., constant fractional error - meaning that large numbers have larger dispersions than do smaller numbers), it is customary to correct the heart rate variability for the underlying heart rate itself, creating an ordered series of DRR /RR plotted against sample number in a temporally ordered sequence. These data are also suitable for "time series" analysis. They may be thought of roughly as a normalized derivative of the raw data.

A question of fundamental physiological and clinical interest concerns the character of the modulation of the time relation of heart beats. For example, data on heart rate and heart rate variability in premature infants have proved valuable as indices of developmental changes and reactivity to stimuli. Similar measures have been used in adults to estimate risk of sudden cardiac death and to predict mortality after acute myocardial infarction [28 - 40].

It is well known that respiratory cycles are coupled to cardiac cycles, with an overall ratio of four heart beats per breath for all members of Class Mammalia. Therefore, the respiratory frequency almost always shows up in a spectral analysis of heart rate data. But beyond the respiratory sinus arrhythmia, as this coupling is called, there is also a broad 1/f spectrum of the heart beat period [41], and other peaks in heart rate spectra have been identified [35, 42]. It has been suggested that these various spectral peaks are associated with thermal regulation, respiration, vasomotor tone alterations and baroreceptor reflexes [42, 43]. But apart from these couplings of heart rate to other near-periodic physiological

processes, there is interest in the residual spectrum after these few peaks are accounted for. Specifically, what is the character of the broad band noise in the background? Particularly, one might ask whether there is a $1/f$ spectral property, as may be typical of chaotic dynamics and as has been reported by Kobayashi and Musha [41]. It is also of interest to know what will happen to heart rate variability in the case of denervation of the heart, as seen after heart transplantation (see [27]).

4.1 Is Heart Rate a State Variable?

Biological state variables may be thought of as those involved in thermodynamic forces and fluxes, whose behaviors strongly affect the overall stability (health) of the system. An example of a macroscopic flux variable is cardiac output; an example of a macroscopic force variable is mean arterial pressure. (Heart rate is a crude estimation of the state variable cardiac output under conditions in which stroke volume is nearly constant, but those conditions are not always sharply defined.) The behavior of a biological state variable reflects at least four influences: (1) developmental influences that act over a lifetime, (2) status influences that operate over months or years, (3) modal influences that have to do with ongoing behavior and operate over seconds to hours, and (4) transients, also operating over seconds to hours. Respective examples might be: (1) developmental lifetime variable - the constraints that a person is a mammalian, human male; (2) status variable - age; (3) modal variable - wakefulness (versus sleep), and (4) a transient variable - exercise or emotion. (Even though heart rate is not a state variable, it responds to the same four influences.)

Many physiological state variables are homeodynamically rather than homeostatically regulated. That is to say that their mean operating behavior is not that of a relatively fixed point or value (homeostasis), but rather that of a generalized limit cycle (orbital stability as a biological rhythm). In the case of a nonstate variable such as heart rate, underlying

homeostatic or homeodynamic regulatory processes may be masked by transients and noise. A major problem in the study of heart rate variability is to determine whether or not it reflects masking influences or underlying physiological state and state changes.

In the case of heart rate, $y(t)$, the following influences might apply:

$y(t) = f(y_1, y_2, \ldots, y_7)$

where y_1 is the allometric relation for mammals -

$$HR\ interval = 0.2\ (body\ weight\ in\ kg)0.25$$

; y_2 carries the influences of the order, family, genus and species; y_3 carries the influence of sex (women have higher heart rates than men for the same conditions); y_4 carries the influence of age; y_5 carries the influence of the recent past, including the lifestyle (e.g., how much coffee is regularly drunk); y_6 reflects the field influence of the ongoing situation (e.g., exercise); y_7 constitutes a wastebasket term, including noise that is unresolvable, plus deterministic or stochastic couplings to other physiological systems such as respiration.

In this analysis items y_1 through y_4 are not negotiable, but fixed for a particular individual at a particular age. Items y_5- y_7 may be altered by lifestyle changes, drug interventions or environmental changes. Most of the variability of heart rate arises from y_6 and y_7, items which are not under internal regulation. Some of the HR variability arises from manipulated variables in the regulation of other aspects of circulatory functions. The linear decline in maximum achievable heart rate with age exemplifies this fact. As Weisfeldt et al. (1984) have clearly shown, cardiac output during (submaximal) exercise is well sustained until about age 80 in subjects without coronary artery or other serious cardiovascular disease, in spite of the fall in maximum or near maximum heart rate. An increase in stroke volume compensates. Cardiac output appears as a defended and regulated variable, but not heart rate.

Sources of heart rate variability include microscopic channel noise in pacemaker currents; temperature fluctuations; environmental chemicals such as caffeine; couplings to respiration; high energy or high mass activities such as exercise, eating, sleep/wake transitions or postural shifts; and low energy/mass inputs that are more "informational", such as being criticized or being embarrassed (i.e., emotional inputs). Viewed this way heart rate variability is seen as being a sort of final common pathway for a wide variety of influences; therefore it will be intrinsically difficult to resolve time series records of heart rate into state assessments, except under very well defined conditions. Such conditions might include anesthesia, strictly controlled environments, and dominant physiological state (rest, fasting). A disadvantage of studying heart rate under such conditions is that its behavior may be irrelevant and there may be poor generalizability beyond the very special conditions under which the measurements were made. Therefore, one is tempted to study heart rate in adults, and some children, under 24 hour or longer monitoring conditions in which the subject is leading his (nearly) usual life.

The questions that concern us are: (1) how do we express and analyze non-lethal heart rate variability and (2) what can be learned from heart rate variability, if it is not a physiological state variable? (Potentially lethal dysrhythmias such as ventricular tachycardia, ventricular fibrillation, or extreme bradycardia and asystole, are clinically important in adults but not really relevant to the issue addressed by this conference.)

4.2 Signal Analysis of Heart Rate Variability

Sayers opens Chapter Three of the Kitney book [31] with this comment on the signal analysis of heart rate variability:

"The beat-by-beat variations of heart-rate are neither quite deterministic nor entirely random and, as with most biological variables, successive periods of lead to somewhat different results - partly because of the operation of changing biological factors, and partly

due to statistical sampling effects (...). The cardiac signal in this context can be regarded as a sequence of point events (occurrences of P or R waves in an ECG) and two types of approach are possible. First, some global features of the point-sequence could be measured. Two such global measures are mean heart-rate and variance of interbeat intervals; this kind of measure certainly reflects the existence of changing physiological conditions, but only in a rather unspecific way (...). Such an approach can indicate nothing about any sequential patterns traced out by successive intervals; but, as far as the heart-rate variable is concerned, these patterns offer the only prospect of any detailed picture of the behavior of underlying physiological mechanisms. Thus, a second type of approach is desirable, that studies pattern features of the fluctuations of heart-rate.

An analysis which draws on the coherent dynamic features of these fluctuations, rather than on their global description, is potentially more likely to illuminate detailed system structure and properties of the underlying physiological mechanisms."

Because of the hyperbolic (inverse) relationship between the time series of interbeat intervals (RR) and the so-called "instantaneous heart rate", one must choose the form of the data for analysis, focusing either on intervals or on rate. At slow heart rates variations in interbeat intervals are not very sensitive indicators of variations in physiological effects; conversely, at high heart rates variations in instantaneous rate are insensitive indicators. One way around this uneven weighting is to use a sequence of interbeat intervals as the primary data, but to express variability as done by Mazza et al. [34], viz. normalize the DRR defined as : $DRR_n = RR_{n+1} - RR_n$ where RR is the time in milliseconds from the peak of one R wave to the next and "n" is the interval number in the ordered set of a time history of the variable. The ratio $\frac{DRR_n}{RR_n}$ normalizes the absolute variability of the heart beat interval to the underlying rate itself and corrects for the linear correlation between DRR and RR which merely expresses the (essentially trivial) fact that in many

natural processes the absolute variability around a mean value increases as the value of the mean itself increases (i.e., many processes naturally tend to have constant fractional error, or coefficient of variation). After the normalization a new time series results that can be analyzed for global statistical properties during different epochs, or that can be subjected to spectral analysis, or treated in more advanced ways such of those of nonlinear mechanics. Whenever spectral analysis is used on a physiological time history it is desirable to create an artificial, control time series by shuffling the ordered set of the original. Shuffling preserves the amplitude distribution but destroys the ordinal relationships. As a result of shuffling the spectrum should be whitened and putative peaks seen in the spectrum of the original time series should disappear (see Odell et al. [44]).

Once the normalized interval measure has been chosen as basic to the representation and analysis of heart rate variability, analytical descriptions such as the serial correlation of intervals, the interval spectrum, and the band-filtered version of the interval sequence all are useful. It is then necessary to decide whether the sample number in the sequence, or time, should be used as the basis for displaying the sequence of events. It is not necessary to convert a series of point events into a form that models the sequence as a continuous underlying signal sampled regularly in time. In practice, such regularization of the sequence of samples turns out to be entirely unimportant, except perhaps when it is required to compare the cardiac signal with some simultaneous ongoing waveform, such as mean arterial blood pressure, with reasonably high precision. But that can be done by basing a cross-spectral analysis or coherence analysis between two time series on a series of sampled numbers, rather than equally spaced sampling times. Ultimately, of course, after a spectral analysis it is desirable to convert any significant "peaks" into some statement about variations in time, in order to scale a problem physiologically. But that can be a last step in the analysis.

4.3 Respiratory Sinus Arrhythmia (RSA) (Respiratory- Circulatory System Coupling)

The importance of the coupling between respiratory periodicities and heart rate variability during development in infants is well illustrated by the work of Mazza, Gordin et al. [34] Katona et al. [45], and Harper et al. [46]. F. Raschke [47] has shown that the strength of coupling between the cardiac and respiratory systems in adults varies with the underlying physiological state. Spectral analysis of a time history of RR intervals in normal young human beings reveals three peaks: 15/min (respiratory frequency), 7/min (changes in mean arterial pressure) and 1/min (thought to represent flow mechanics of the arterial system itself). In young subjects studied on a low protein diet at constant bed rest in a constant environment, there is no clear circadian rhythm in RR interval, but during sleep the distribution of periods is much narrower. The cardiovascular system has less variance during sleep in adults, as in infants.

The coupling between the respiratory and cardiac systems has been expressed as a phase coordination between a preceding R wave and inspiratory onset [48]. The coupling is tightest during sleep; it is moderate during restful wakefulness when the RSA shows as a frequency modulation of heart rate, as expected. However, the two systems are entirely decoupled during exercise - the relationship between them is then random. These various degrees of coupling represent physical and hemodynamic constraints at the lowest level, vagal-induced reflex coordination at the middle level, and central coordination at the highest level. During exercise in untrained individuals a coupling between inspiration/expiration respiratory cycling and the rhythm of walking or running is moderately strong; as athletic training is increased, the coupling becomes tighter between these two oscillatory behaviors, while the coupling between respiration and cardiac cycles is weakened. We cite Raschke's work merely as an example of the fact that coupling strengths between the cardiovascular and the respiratory systems vary with physiological state in adults, as

well as in infants. Thus, a raw estimate of RSA, without providing some context, will be insufficient for interpretation. An independent measure not involving respiration or circulation is needed to define the state context in which RSA strength can be meaningfully interpreted. There is no agreement on what that additional state information should be.

4.4 Is There a Chaotic Attractor that can be Revealed by Dimensional Analysis of Heart Rate Variability?

The modern techniques of analysis of nonlinear dynamical systems [5] are just beginning to be applied to time histories of normal heart rate data. These approaches emphasize lag plots, mutual information, and the search for an attractor and its dimension, that would be characteristic of a physiological "state." The state can be gross, merely sleep vs. wakefulness, or it might be more refined to encompass the minor states of eating, exercise, sexual activity, etc. An example of an analysis of the heart rate record from a normal 35-year old woman (obtained from a time segment of a 24 hour Holter monitor recording) is discussed in section 2 above. This segment corresponds to the time of $n_{data} = 828$ heart beats recorded during normal activity. Since perturbations in the recording are unavoidable this also corresponds to the limit of contiguous data segments. The results from a later data segment indicate that the fluctuation of dimensionality is of the order of $\Delta d \approx 0.5$ which corresponds to a relative change of about 10%.

As one possibility for increasing the number of data points we make the assumption that both segments are generated by the same dynamical system and therefore the reconstructed vectors lie on the same attractor. Therefore we can compute the dimension from both sets as long as we make sure that the reconstruction is done properly, i.e. without mixing of the segments. The results are shown in fig.17 for the combination of two segments of $n_{data,1} = 828$ and $n_{data,2} = 752$ where we plot the dominant dimension as a function of the embedding dimension. Note the better convergence and smaller errors compared to the

single segment data of fig. 8 ($d_{AP} = 5.8 \pm 2.4$ for the first segment, $d_{AP} = 5.6 \pm 1.6$ for the second segment, and $d_{AP} = 4.8 \pm 1.9$ for the combination of the two segments. In fig. 18 we see that the histogram is more normal compared to that of fig. 7. With this and similar improvement it might turn out that dimension estimation has its own value as diagnostic tool.

3. Muscle tremor

The neuronal activity and the time course of excitation within the human nervous system (especiall the motor system) leads to minute oscillatory motions of the whole organism or parts of it, which normally are in an order of magnitude far below perception thresholds of our (e.g. visual or acoustic) sensory organs. This vibratory output of the CNS shows frequencies ranging from approx. $1 - 120\ Hz$ and is usually classified as body sway ($1 - 3\ Hz$), different (limb- or finger-) tremors ($6 - 16\ Hz$, max. $< 25\ Hz$) including eye tremor ($< 120\ Hz$) and as muscle tremor or vibration ($1 - 100\ Hz$), which is of special interest in this context. The latter is mainly based on the phaenomenon of electro-mechanical coupling: Electrical impulses (spikes) of the motor system are converted in mechanical "ripples" (twitch contractions) of the related single muscle fibres, which are connected to the innervating motor neurons via neuro-muscular junctions. This mechanism leads to a muscular vibration pattern, which mainly resembles the firing statistics of related motor units. Indeed, spectral analysis (by FFT) of such "vibromyogram" (VMG) reflecting the mechanical gross activity of a skeletal muscle reveals frequency peaks similar to the mean rhythmicity of spike discharge rates described in single unit studies [49]. Other possible mechanisms underlying endogenous muscular vibrations are discussed elsewhere more thoroughly [49]. In the presented study concerning muscle oscillations the following questions have been addressed: (i) Is the complexity of the mechanical spinal CNS output (VMG) comparable to that of the supraspinal electrical CNS output (EEG)?

(ii) Are the complexity parameters of the VMG stable observables. (iii) Does the VMG-signal's complexity vary with the functional state of the muscle comparing relaxation with isometrical contraction? (iiii) Do lesions of the CNS, for instance caused by unilateral cerebral infarctions affect the dimensionality of the oscillation pattern of the paretic (and spastic) muscles? Tibialis and biceps muscles were investigated at rest and during isometrical contraction. The muscle vibrations were recorded with an accelerometer attached to the skin overlying the muscle of interest. The subjects and patients were lying in a supine position with eyes closed. Different constant levels of force had to be maintained over 4 minutes. Oscillations of the non-contracted muscles exhibited a low dimensional 'chaos' with a (Grassberger-Procaccia) dimensionality of $D \approx 4$. Such resulting dimensionality of a vibromyogram obtained from a 'resting' right biceps muscle is shown in fig.19 ($d_{GP} = 4.4 \pm 2.4$ at a goodness of fit $GF = 0.12$). Investigating the time course over 4 minutes by analyzing successive 20 sec segments a remarkable constancy of the dimensionality became evident (fig.20). In fig. 21 we show the sequence of pointwise dimension values which yield an average of $d_{AP} = 4.3 \pm 1.4$. (see fig. 22 for the histogram; note the difference to figs. 7, 13, 18). The good agreement with d_{GP} could indicate a low non-uniformity of the system [11].

In contrast, during isometrical contraction of the same biceps muscle (load of 30 Newton) higher dimensional chaos occurred. It was paralleled by an increase in dimensionality up to $d_{GP} \approx 8$. The corresponding spectral array can be found in ref. [49].

In patients with spastic hemiparesis caused by a contralateral cerebral infarction intra-individual side-differences in the dimensionality (up to a $\Delta D \approx 3$) of bilateral muscle oscillations simultaneously recorded could be found [to be published]. This change in complexity may be due - among others - to a 'pathological' mode of motor unit activity [50,51]. The increase of the dimensional complexity of muscle vibrations during contraction

seems to be reasonable as the whole 'motor maschinery' of the nervous system is coming into play. Thus, the preliminary results point out the predominant role of supraspinal CNS influences to the chaos dimensionality of the muscular vibratory output. The disclosed 'range of entropy' seems to be a general feature of the human CNS activity as the order parameters of the 'mechano-spinal' VMG correspond to dimensionalities of the 'electro-cortical' EEG output [17-24].

Because of the preliminary nature of the results it is too early to draw definite conclusions. But so far, they suggest a pragmatic value of chaos analysis in basic research and clinical applications as methods of non-linear dynamics seem to determine characteristics of (vibratory) biosignals, which are related to different (patho-)physiological states and which cannot be disclosed by conventional analysis-techniques.

References

1. *Journal* M.C. Mackey, L. Glass, *Science* 197, 287, (1977)

2. *Edited Book Perspectives in Biological Dynamics and Theoretical Medicine*, S.H. Koslow, A.J. Mandell, M.F. Shlesinger (Eds.), Annals of the New York Academy of Sciences Vol. 504, New York, 1987

3. *Edited Book Temporal Disorder in Human Oscillatory Systems*, L. Rensing, U. an der Heiden, M.C. Mackey (Eds.), Springer Series in Synergetics, Vol. 36, Springer-Verlag Berlin, Heidelberg 1987

4. *Talk*, A. Gevins, talk given at: *Brain activity as a dynamical system*, Workshop, Pecos Ranch, 1987

5. *Edited Book Dimensions and Entropies in Chaotic Systems*, G. Mayer-Kress, (ed.) Springer Series in Synergetics, Vol. 32, Springer-Verlag Berlin, Heidelberg 1986

6. *Journal* N.H. Packard, N.H., J.P.Crutchfield, J.D.Farmer, R.S.Shaw, *Geometry From a Time Series*, Phys. Rev. Lett. 45: 712, 1982

7. *Book* R.S. Shaw, *The Dripping Faucet as a Model Chaotic System*, Aerial Press. Santa Cruz, CA, 1985

8. *Journal* A.M. Fraser, H.L. Swinney, Phys. Rev. A 33: 1134-1140, 1986

9. *Journal* J.D. Farmer, E. Ott, J. A. Yorke, Physica 7D:153-180, 1983

10. *Journal* P.Grassberger, I. Procaccia, Physica 9D: 189, 1983

11. *Journal* J.S. Nicolis, G. Mayer-Kress, G. Haubs, Z. Naturforsch. 38a, 1157 (1983)

12. *Edited Book, An Approach to Error Estimation in the Application of Dimension Algorithms*, J. Holzfuss, G.Mayer-Kress, in [5]

14. *Journal* D.S. Broomhead, G.P. King, Physica 20D, 217, 1986

15. *Journal* D.S. Broomhead, R. Jones, G.P. King, *Topological Dimension and Local Coordinates from Time Series Data*, Preprint 1987

16. *Journal* K. Geist, G. Mayer-Kress, to be published

17. *Edited Book, Problems Associated with Dimensional Analysis of Electro-Encephalogram Data*, S.P. Layne, G. Mayer-Kress & J. Holzfuss, in [5]

18. *Edited Book*, A. Babloyantz, A. Destexhe, Proc. Natl. Acad. Sci. Vol. 83, 3513, 1986

19. *Edited Book*, A.M. Albano, et al., *Lasers and Brains: Complex Systems with Low Dimensional Attractors", In [5].*

20. Journal A. Cenys, K. Pyragas, Estimation of the Number of Degrees of Freedom from Chaotic Time Series, Preprint Vilnius, 1987

21. Journal I. Dvorak, J. Siska, On some Problems Encountered in Calculating of the Correlation Dimension of the EEG, Preprint Prague 1987

22. Talk W. Freeman, talk presented at Brain activity as a dynamical system, Workshop, Pecos Ranch, 1987

23. Edited Book, Dimensionality of the Human Electro- Encephalogram, G. Mayer-Kress, S.P. Layne, in [2].

24. Edited Book, Analysis of the Human Electroencephalogram with Methods from Nonlinear Dynamics, G. Mayer-Kress, J. Holzfuss in [3].

25. Book, H. Haken, "Synergetics- an Introduction", Springer Series in Synergetics, Vol. 1). Springer-Verlag., Berlin, Heidelberg, 1977.

26. Edited Book, Application of dimension algorithms to experimental chaos, G. Mayer-Kress, to app. in "Directions in Chaos", Hao Bai-lin (Ed.), World Scientific Publishing Company, 1987

27. Edited Book, Dimensional Analysis of Heart Rate Variability in Heart Transplant Recipients, J. P. Zbilut, G. Mayer-Kress, K. Geist, this volume.

28. Journal Sudden infant death syndrome: abnormalities in short term fluctuations in heart rate and respiratory activity, Gordon, D., R. J. Cohen, D. Kelly, S. Akselrod and D. C. Shannon, J.Pediat. Research (in press)

29. Edited Book, Cardiorespiratory and state control in infants at risk for the sudden infant death syndrom, Harper, R. M. Chapter 1 in: Sleep Disorders: Basic and Clinical Research, Spectrum Publications, Inc., pp. 1-27., (1983)

30. Journal Polygraphic studies of normal infants during the first six months of life. I. Heart rate and variability as a function of state, Harper, R. M., T. Hoppenbrouwers, M. B. Sterman, D. J. McGinty and J. Hodgman Pediatric Research 10:945-951, (1976)

31. Edited Book, The Study of Heart Rate Variability Kitney, R. I. and O. Rompelman (Eds.), Oxford University Press, Oxford (1980)

32. Journal Decreased heart rate variability and its association with increased mortality after acute myocardial infarction, Kleiger, R. E., J. P. Miller, J. T. Bigger, Jr., and A. J. Moss, Am. J. Cardiol. 59: 256-262, (1987)

33. Journal Diagnosis and quantification of arrhythmias using an improved R-R plotting system, Lopes, M. G., J. W. Fitzgerald, D. C. Harrison and J. S. Schroeder, Am. J. Cardiol. 35: 816-823, (1975)

34. Journal Relation of beat-to-beat variability to heart rate in normal sleeping infants, Mazza, N. M., M. A. F. Epstein, G. G. Haddad, H. S. Law, R. B. Mellins and R. A. Epstein, Pediatric Research 14: 232-235, (1980)

35. Journal A 90-min cardiac biorhythm: methodology and data analysis using modified periodograms and complex demodulation, Orr, W.C. and H. J. Hoffman, IEEE Trans. on Biomed. Eng., BME-21: 130-143, (1974)

36. Edited Book, Spectral analysis of fetal heart rate: a potential method for the detection of fetal distress, Porges, S.W., Chapter 2 in: Infants Born at Risk, T. M. Field (ed.), Spectrum, New York, pp. 17-27, (1979)

37. Journal The statistical analysis of heart rate: A review emphasizing infancy data, Richards, J.E., Psychophysiology 17: 153-166, (1980)

38. Journal Descriptors of the rhythmicity in respiration and heart beat of newborn infants, Scholten, C.A. and J.E. Vos, Medical and Biological Engineering and Computing 19: 83-90, (1981)

39. Journal Comparative investigation of the mathematical properties of some descriptors for biological point processes: examples from the human newborn, Scholten, C.A. and J.E. Vos, Medical and Biological Engineering and Computing 20: 89-93, (1982)

40. Journal Compiled profile of respiration, heart beat and motility in newborn infants: a methodological approach, Scholten, C.A., J. E. Vos, and H. F. R. Prechtl, Medical and Biological Engineering and Computing 23: 15-22, (1985)

41. Journal 1/f fluctuation of heart beat period, Kobayashi, M. and T. Musha, IEEE Trans. on Biomedical Engineering 29: 456-457, (1982)

42. Journal Power spectrum analysis of heart rate fluctuation: a quantitative probe of beat-to-beat cardiovascular control, Akselrod, S., D. Gordon, F.A. Ubel, D.C. Shannon, R.J. Cohen, and A.C. Barger, Science 213: 220-224, (1981)

43. Journal Influence of cardiac neural inputs on rhythmic variations of heart period in the cat, Chess, G.F., H.K. Tam, F.R. Calarescu, Am. J. Physiol. 228: 775-780, (1975)

44. Journal A permutation test for periodicities in short, noisy time series, Odell, R.H., S.W. Smith and F.E. Yates, Ann.Biomed. Eng. 3: 160-180, (1975)

45. Journal Maturation of cardiac control in full-term and preterm infants during sleep, Katona, P.G., A. Frasz and J. Egbert, Early Human Development 4: 145-159, (1980)

46. Journal Development of sinus arrhythmia during sleeping and waking states in normal infants, Harper, R. M., D. O. Walter, B. Leake, H.J. Hoffman, G. C. Sieck, M. B. Sterman, T. Hoppenbrouwers and J. Hodgman, Sleep 1: 33-48, (1979)

47. Edited Book, Coordination in the circulatory and the respiratory systems, Raschke, F. , pp. 152-159 in [3]

48. Edited Book, The hierarchical order of cardiovascular- respiratory coupling, Raschke, F., In: Cardiorespiratory and Cardiosomatic Psychophysiology, P. Grossman, K. H. L. Janssen, D. Vaitl (Eds.), Plenum Press, New York, (1986)

49. Journal The Computer-Vibromyography as a new tool in studying muscle function, Keidel M., Keidel W.-D. submitted to publication

50. Journal Abnormal vibromyogram spectra in motor disorder Keidel M., Flick Th., Tirsch W.S. Electroenceph.clin.Neurophysiol.66(5)S122

51.Edited Book Computer-aided detection of temporal patterns in human CNS dynamics, Tirsch W.S., Keidel M., Pöppl S.J. , In: Proceedings of the international working conference: progress in biological function analysis by computer technologies, May 19-23,1987, ed. by J.L.Willems. North-Holland Publishing Company.

4. Edited Book Studying temporal order in human CNS by "running" frequency and coherence analysis, Keidel M., W.-D. Keidel, Tirsch W.S., Pöppl S.J., pp. 69-78 in [3]

Figure Captions

Fig. 1: Time series and planar state space reconstruction from inter beat intervals of a heart of a healthy female, taken during regular daily activity with the help of a Holter monitor. The delays in the reconstructions are $k = 1$ and $k = 4$.

Fig. 2: A series of gauge functions in a log-log representation for embedding dimensions $1 < n < 20$ for the same heart data as in fig.1. We see for small values of $log\ r$ the effect of the finite resolution of the measurement ($\approx 1\%$). The solid line indicate the fit region for each embedding dimension determined by the algorithm.

Fig. 3: Selected scaling ranges for dimension estimation of the data of fig. 1. The solid lines corresponds to a goodness of fit of $GF = 0.2$.

Fig. 4: Pointwise dimension $d_{\vec{\xi}_j}$ vs. index j. Since we have $n_{data} = 828$ interbeat intervals, the reference points $\vec{\xi}_j$ are separated by roughly four heart beats. The errorbars indicate the goodness of fit relative to a value $GF = 0.2$ indicated in the inset. For reference points which reached this value we did not plot errorbars. The initial lenght of the fit region corresponds to a scale factor $\alpha = \frac{r_{max}}{r_{min}} = \sqrt{2}$. The embedding dimension is $n = 20$.

Fig. 5: Same as in fig. 2 after singular value decomposition with windowlength 100.

Fig. 6: Same as in fig. 3 after singular value decomposition.

Fig. 7: Histogram for the data of fig. 3 (solid lines) and for fig. 5 (dotted lines).

Fig. 8: Estimated dimension value $< d_{\vec{\xi}_j} >_{\vec{\xi}_j}$ vs. embedding dimension n. The error bars correspond to to the standard deviation of the dimension distribution and are solid lines for the original data and broken lines after singular value decomposition. Same data and parameters as above.

Fig. 9: Percentage of reference points which reach a certain goodness of fit GF as a function of GF and embedding dimension n. (Same scale factor as in fig. 3, no SVD)

Fig. 10: Dominant dimension as a function of the goodness of fit GF and embedding dimension n. Same data and parameters as above.

Fig. 11: Same as in fig. 9 after SVD.

Fig. 12: Standard deviation of dominant dimension as a function of the goodness of fit GF and embedding dimension n (same condition as fig.).

Fig. 13: same as fig. 6 but here we can see how the observed histogram depends on the embedding space. (dotted line corresponds to fig. 7)

Fig. 14: Observed dimension of eeg data before anesthesia as a function of the embedding dimesnion and teh goodness of fit (GF).

Fig. 15: Same as fig. 8 for eeg data before anesthesia. ($GF = 0.1$, scale factor $\alpha = 2.0$)

Fig. 16: Same as fig. 15 during medium fluroxene anesthesia.

Fig. 17: Same as in fig. 8 for the concatenation of two data segments of length $n_{data,1} = 828$ and $n_{data,2} = 752$.

Fig. 18: Histogram for the data of fig. 17. (same parameter as in fig. 7)

Fig. 19: Grassberger-Procaccia dimension for non-contracted biceps muscles. ($n_{data} = 10^5$, $GF = 0.12$, $\alpha = 2$, sampling rate $\omega = 500Hz$)

Fig. 20: Sequence of dimension values of successive segments of $n_{data,i} = 10^4$ datapoints.

Fig. 21: Sequence of pointwise dimension values for data of fig. 19.

Fig. 22: Histogram of data of fig. 21 (note the difference to figs. 7, 13, 18).

Fig 1

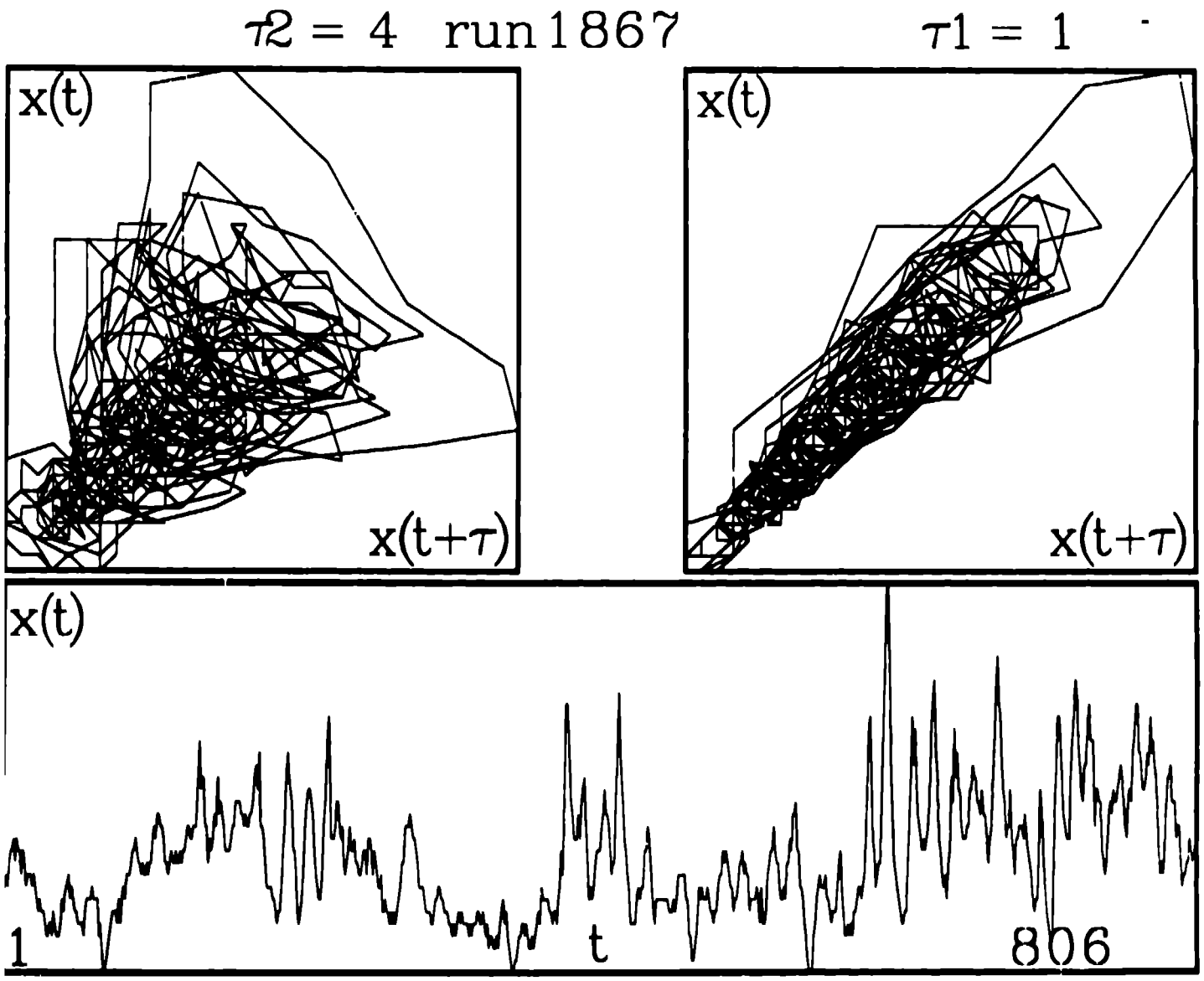

1FILE: SP18670 KREF:100

NSEG : 1	NOTOT : 828	NDAT : 743
NREF : 200	KREF : 100	FITGUE: 0.20
BNU1 : 4	NDELAY: 4	NWIND : 4

NO SING. VALUE DECOMPOSITION

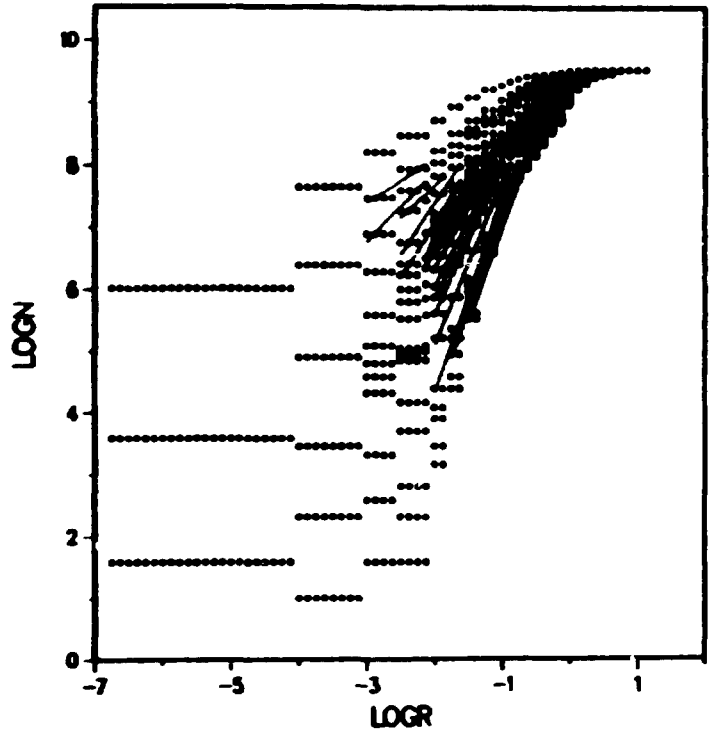

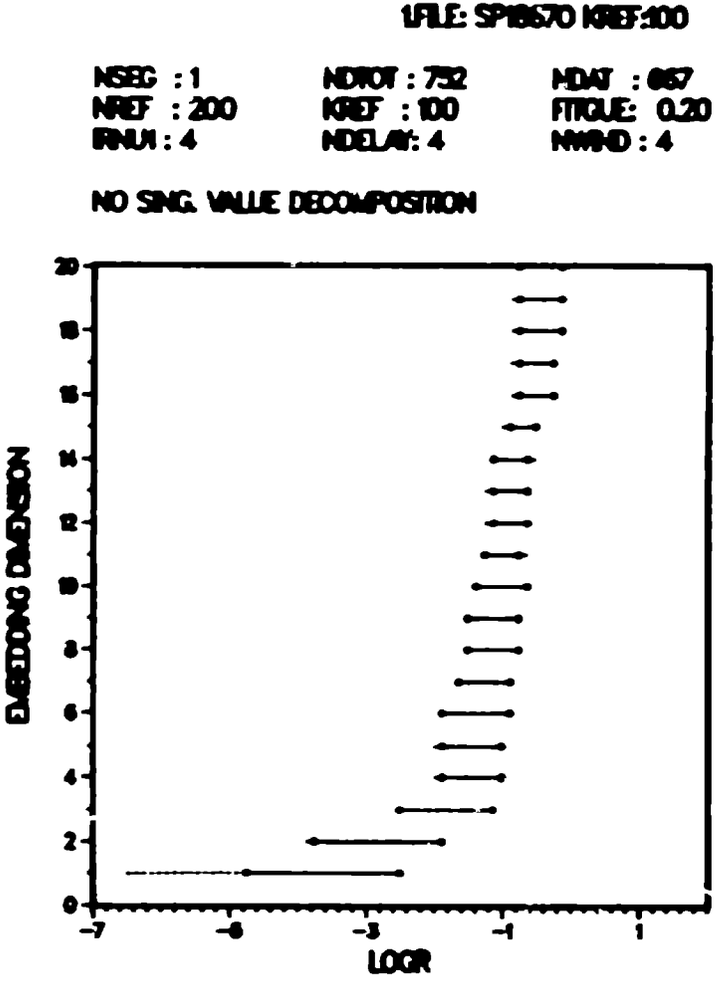
1FILE: SP18670 KREF:100
NSEG : 1
NDROT : 752
NDAT : 667
NREF : 200
KREF : 100
FTOLE: 0.20
NNUM : 4
NDELAY: 4
NWIND : 4
NO SING. VALUE DECOMPOSITION
EMBEDDING DIMENSION
0
2
4
6
8
10
12
14
16
18
20
-7
-5
-3
-1
1
LOGR

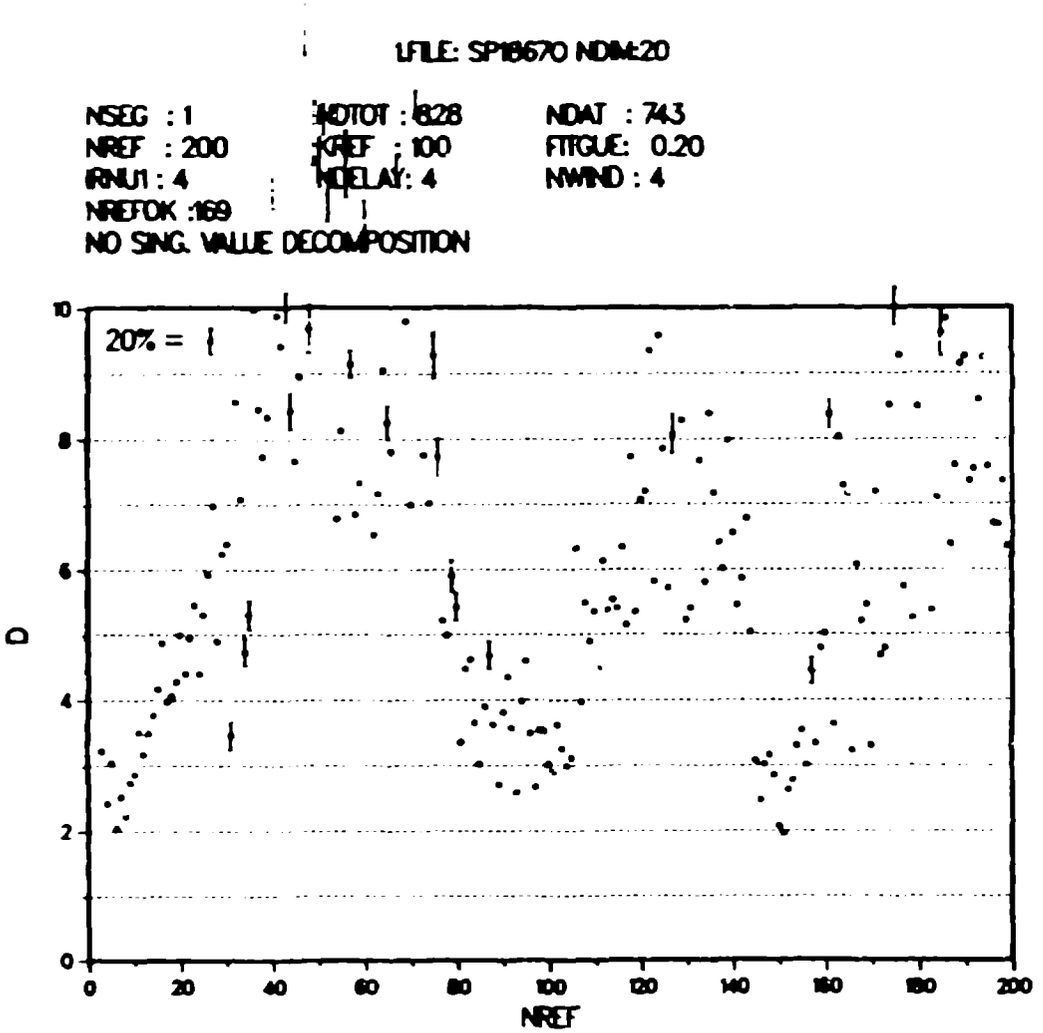
LFILE: SP18670 NDIM:20
NSEG : 1
NREF : 200
IRNU1 : 4
NREFOK :169
NO SING. VALUE DECOMPOSITION
NDTOT : 828
KREF : 100
NDELAY: 4
NDAT : 743
FITGUE: 0.20
NWIND : 4
20% =
D
NREF
0
2
4
6
8
10
0
20
40
60
80
100
120
140
160
180
200

fig 5

1FILE: SP1867BIKREF:100

NSEG : 1	NDTOT : 828	NDAT : 720
NREF : 200	KREF : 100	FITGUE: 0.20
IRNU1 : 4	NDELAY: 1	NWIND : 4

SING .VALUE DECOMP. BY COV. MATRIX

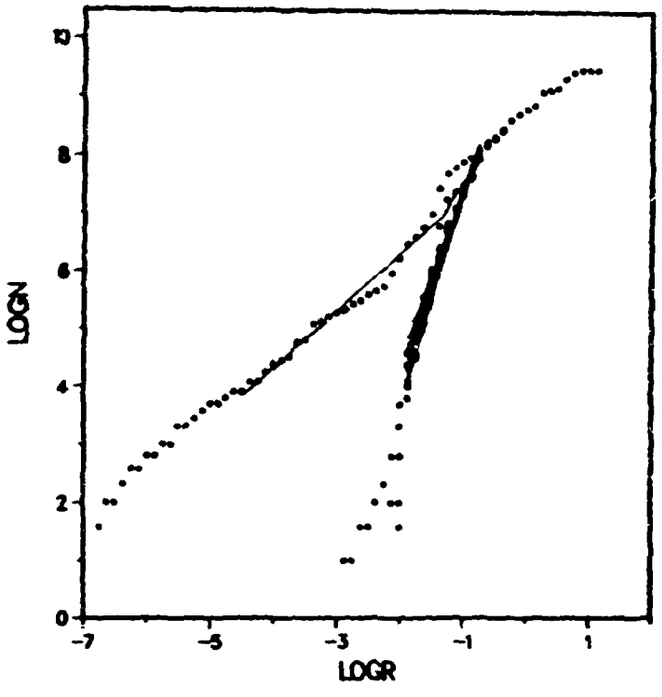

1FILE: SP1867BINDIM:20

NSEG : 1 NDTOT : 828 NDAT : 720
NREF : 200 KREF : 100 FITGUE: 0.20
IRNU1 : 4 NDELAY: 1 NWIND : 4
NREFOK :197
SING .VALUE DECOMP. BY COV. MATRIX

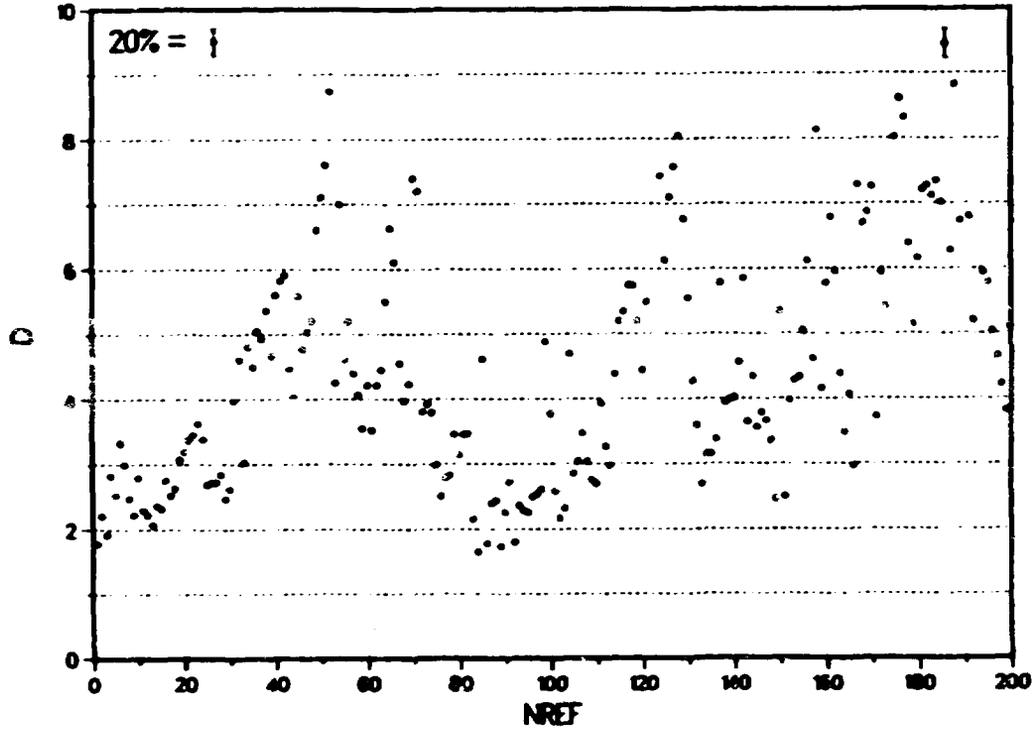

E - 7

p1867p1

2.FILE: [illegible] DIM:20

NSEG : 1	NDTOT : 828	NDAT : 743
NREF : 200	KREF : 100	FITGUE: 0.20
IRNU1 : 4	NDELAY: 4	NWIND : 4
NREFOK :170	DIM20: 5.80	STA20: 2.35

NO SING. VALUE DECOMPOSITION

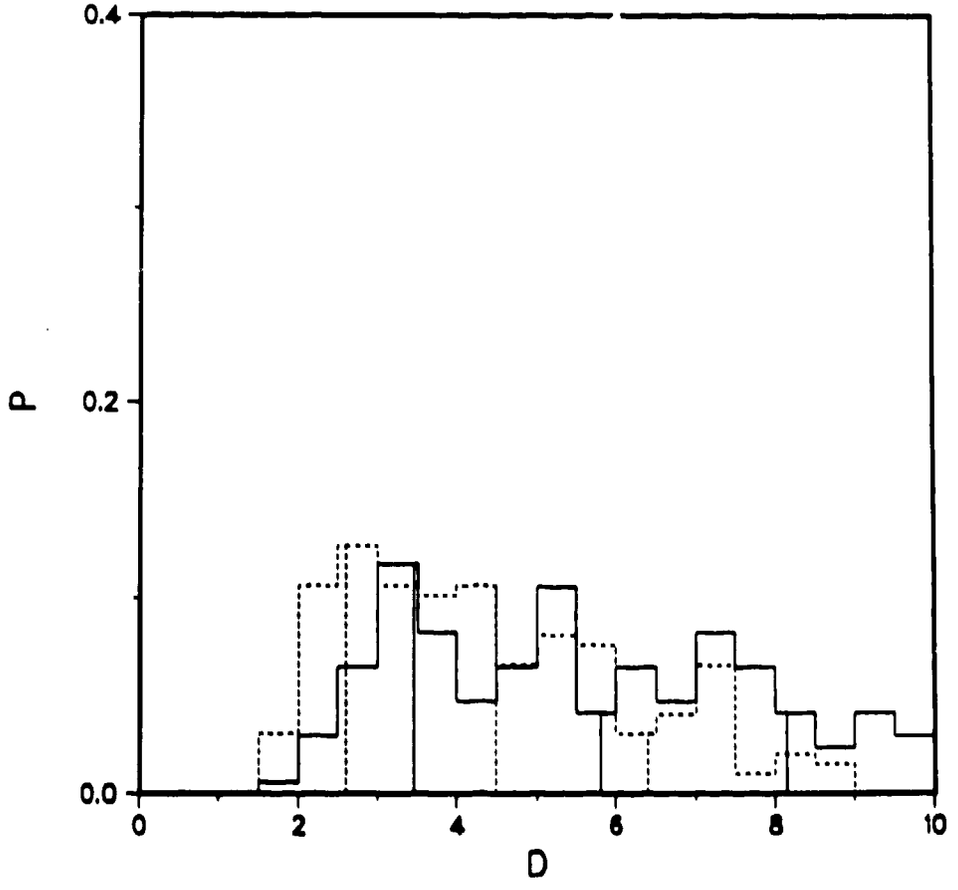

Fig 8

D1867 p1

2.FILE: SR1867B18670

NSEG : 1 NDTOT : 828 NDAT : 743
NREF : 200 KREF : 100 FITGUE: 0.20
IRNU1 : 4 NDELAY: 4 NWIND : 4
NREFOK :170 DIM20: 5.80 STA20: 2.35
NO SING. VALUE DECOMPOSITION

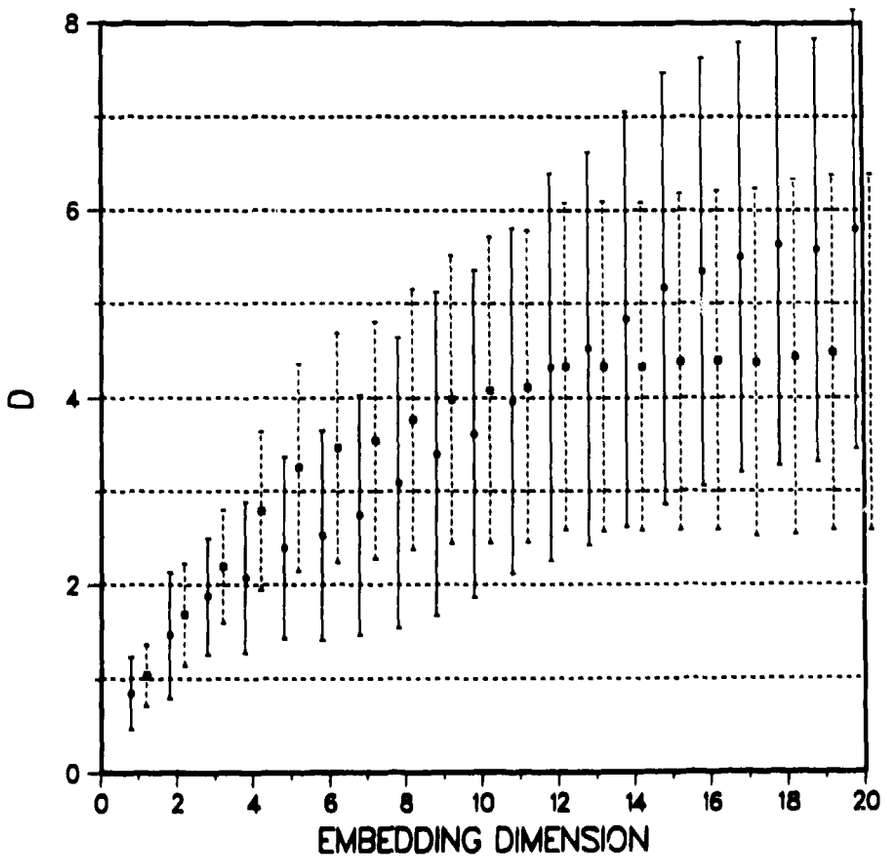

Fig 8 9

Sp 1167

I.FILE: SP18670

NSEG : 1 NDTOT : 828 NDAT : 743
NREF : 200 KREF : 100 FITGUE: 0.20
IRNU1 : 4 NDELAY: 4 NWIND : 4

NO SING. VALUE DECOMPOSITION

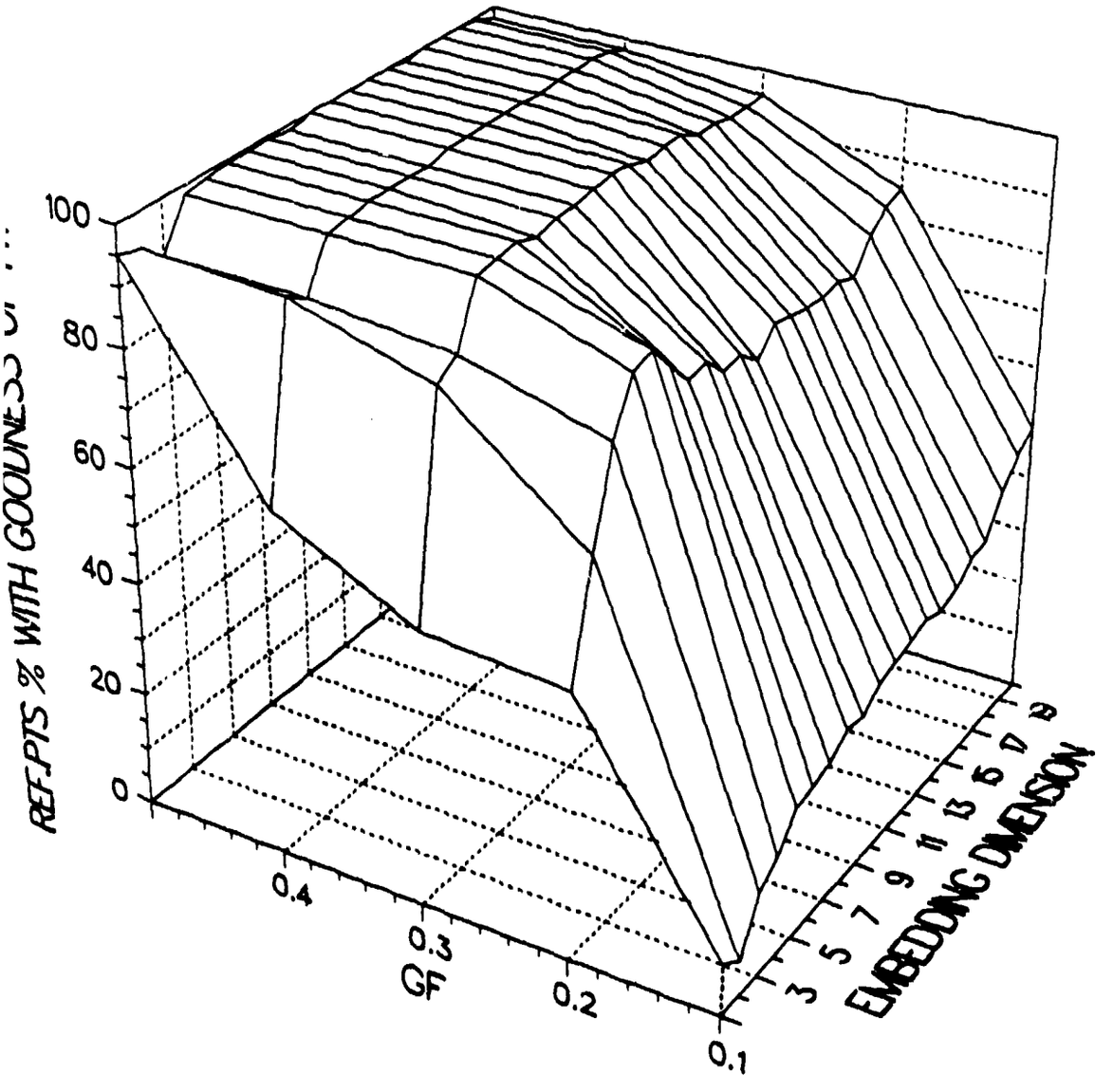

Fig 10

I.FILE: SP18670

NSEG : 1 NDTOT : 828 NDAT : 743
NREF : 200 KREF : 100 FITGUE: ~~0.50~~ 0.2
IRNU1 : 4 NDELAY: 4 NWIND : 4

NO SING. VALUE DECOMPOSITION

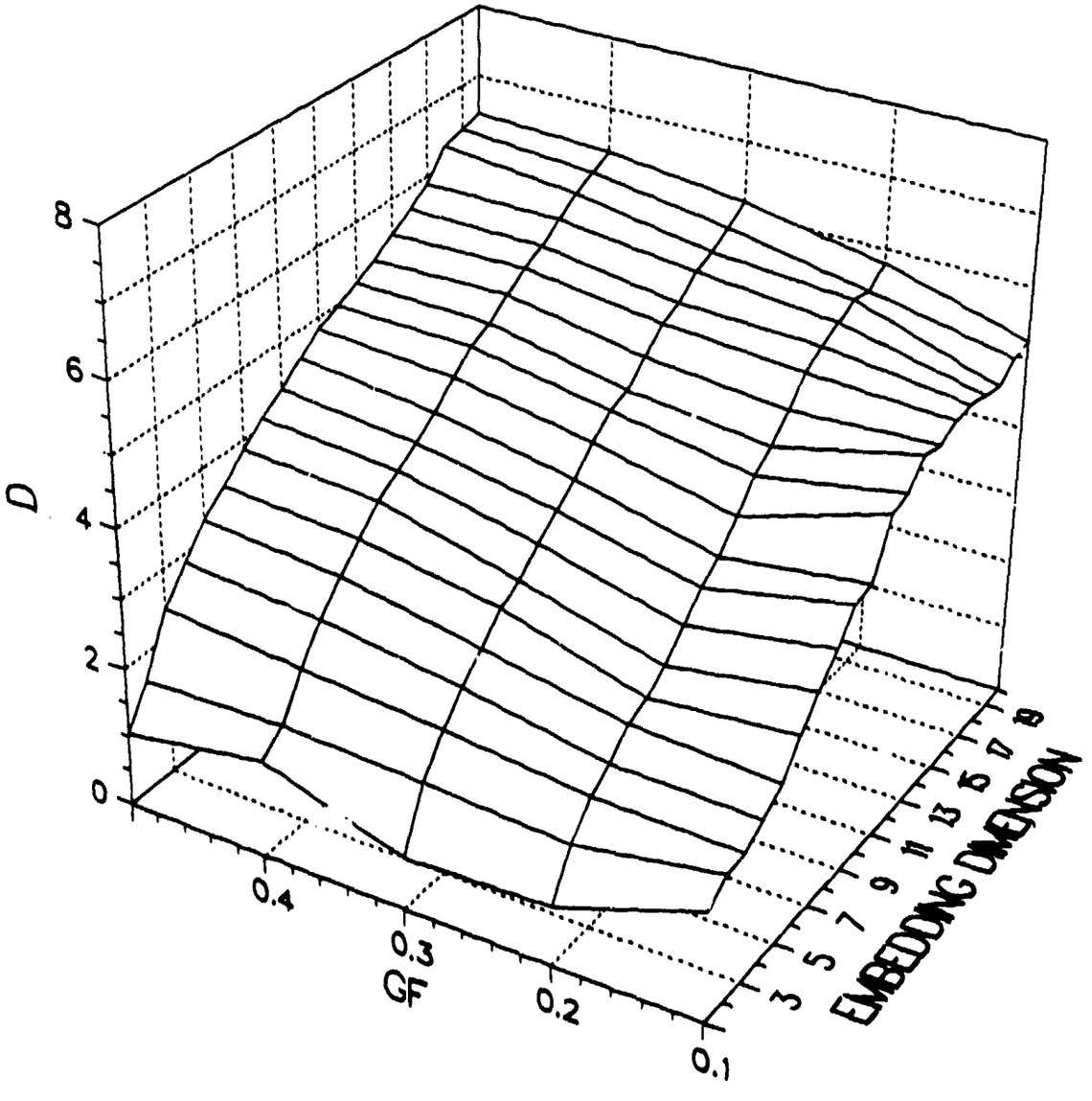

UFILE: SP1867BT

NSEG : 1	NOTOT : 828	NDAT : 720
NREF : 200	KREF : 100	FITGUE: 0.50
IRNU1 : 4	NDELAY: 1	NWIND : 4

SING .VALUE DECOMP. BY COV. MATRIX

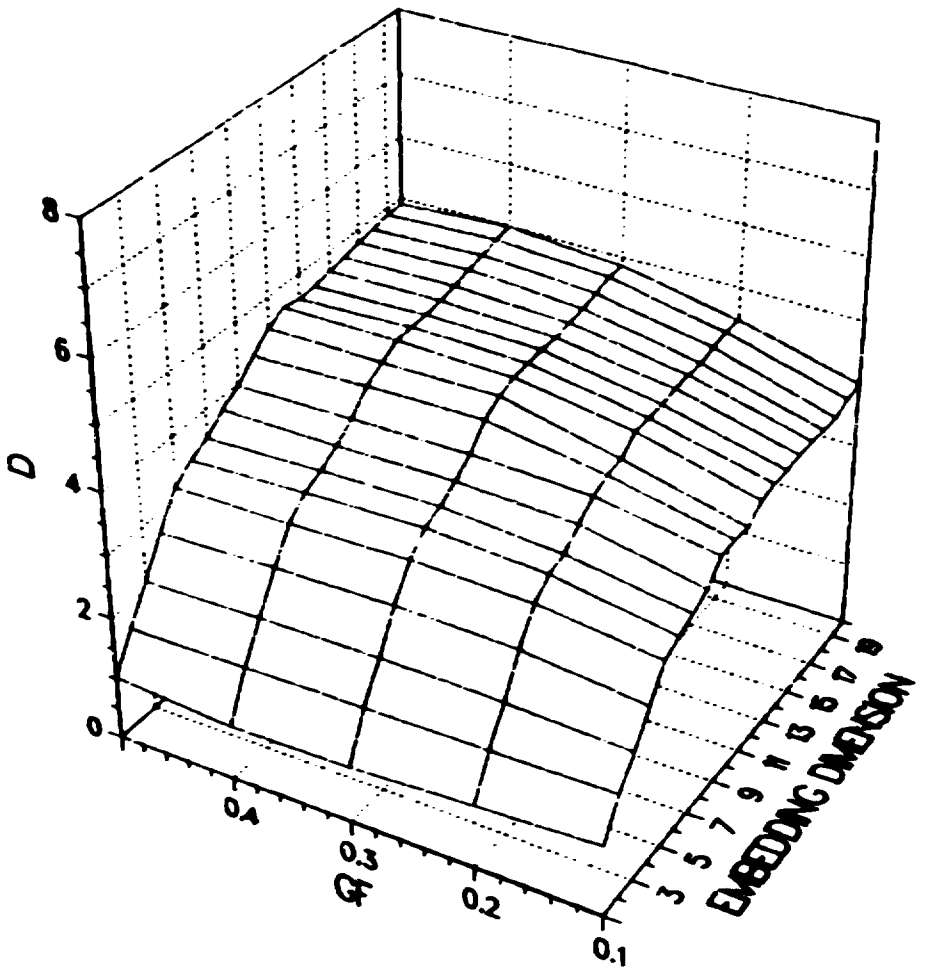

Fig 12

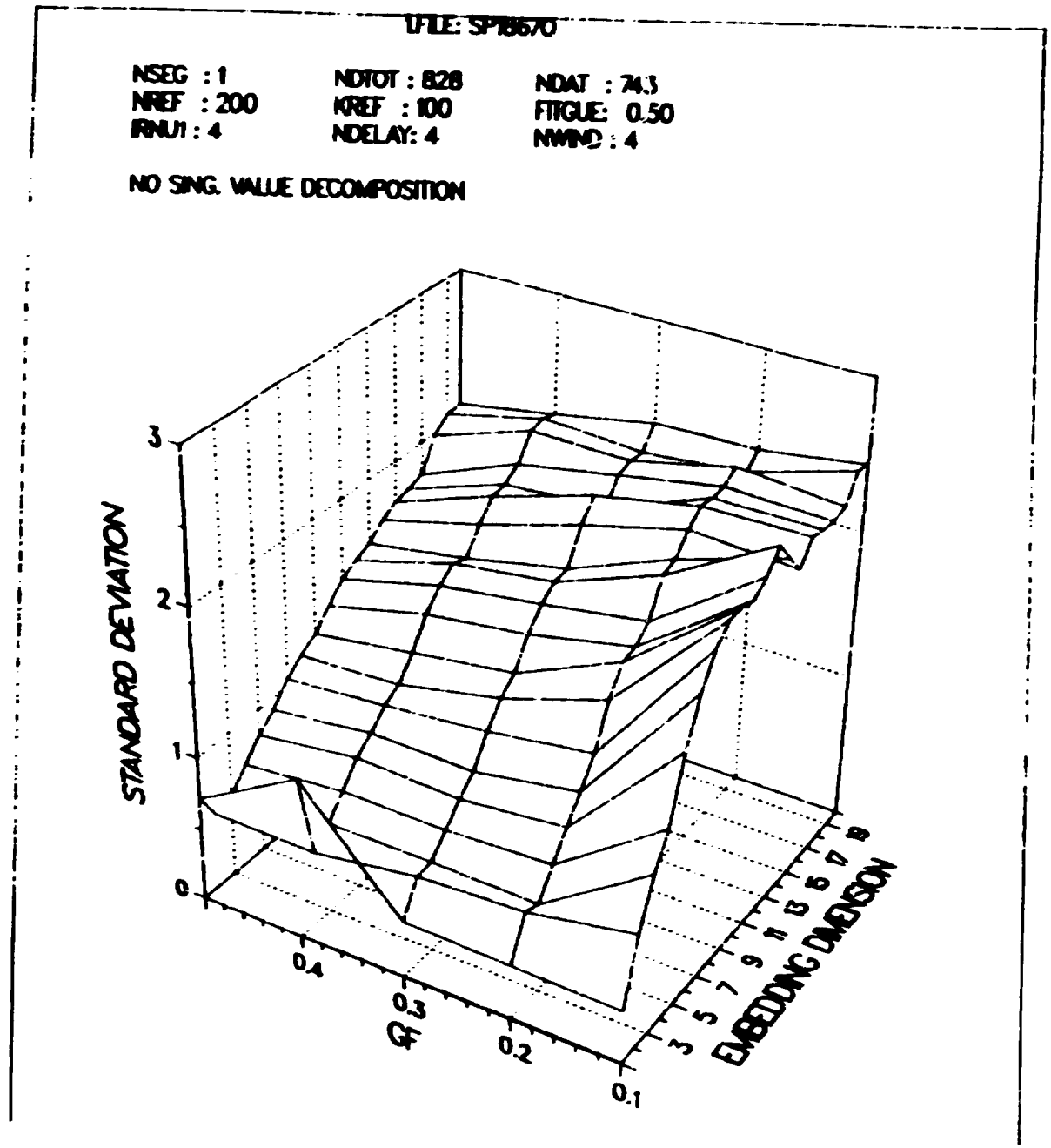
FILE: SP1867C
NSEG : 1
NREF : 200
IRNU1 : 4
NDTOT : 828
KREF : 100
NDELAY: 4
NDAT : 743
FTIGUE: 0.50
NWIND : 4
NO SING. VALUE DECOMPOSITION
STANDARD DEVIATION
0
1
2
3
0.4
0.3
0.2
0.1
3 5 7 9 11 13 15 17 19
EMBEDDING DIMENSION

Fig. 13

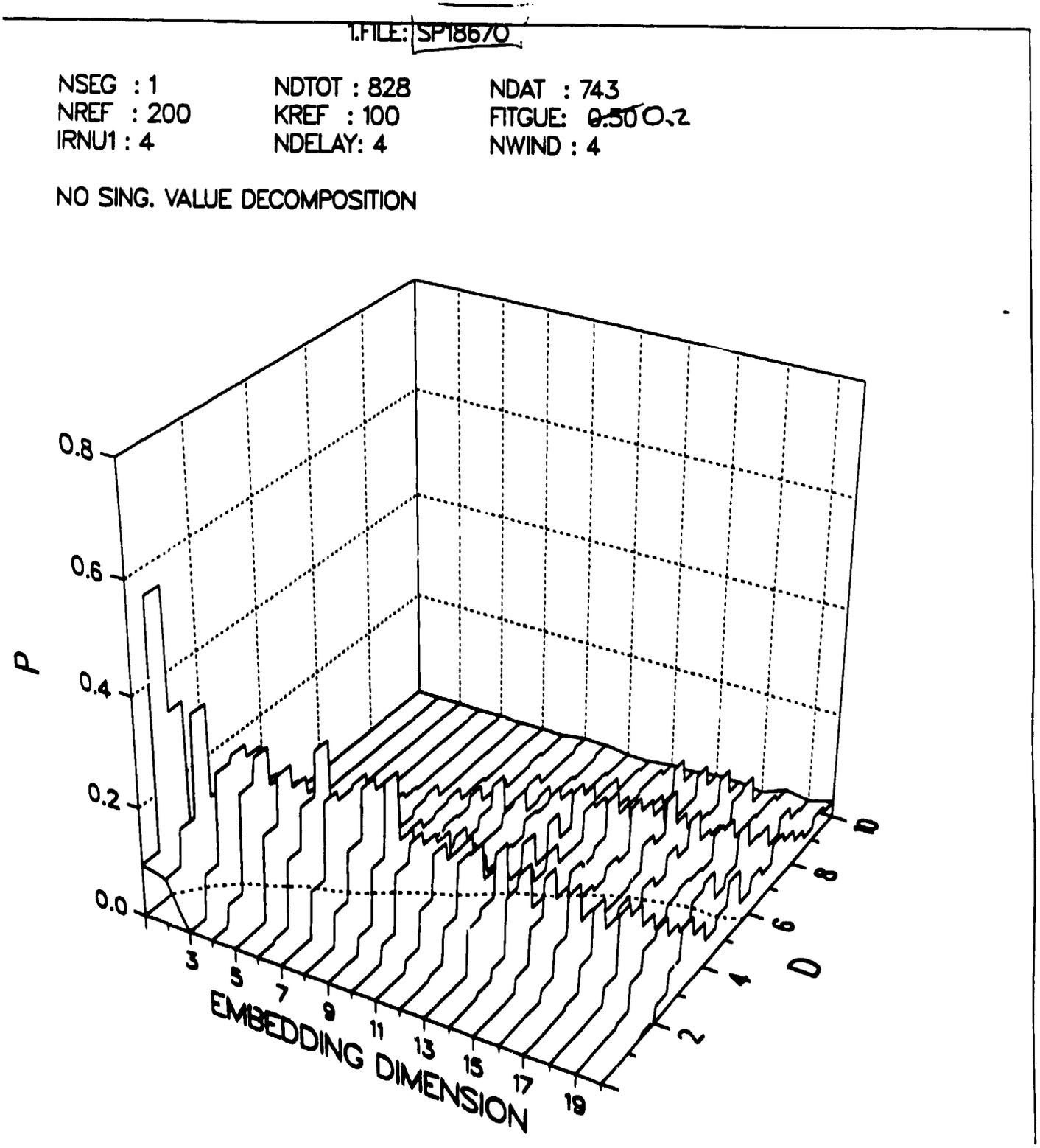
T.FILE: SP18670
NSEG : 1
NDTOT : 828
NDAT : 743
NREF : 200
KREF : 100
FITGUE: 0.50 0.2
IRNU1 : 4
NDELAY: 4
NWIND : 4
NO SING. VALUE DECOMPOSITION
P
0.8
0.6
0.4
0.2
0.0
3
5
7
9
11
13
15
17
19
EMBEDDING DIMENSION
0
2
4
6
8
10
D

T.FILE: SPH40

NSEG : 1	NDTOT : 15360	NDAT : 15142
NREF : 200	KREF : 100	FITGUE: 0.50
IRNU1 : 8	NDELAY: 11	NWIND : 4

NO SING. VALUE DECOMPOSITION

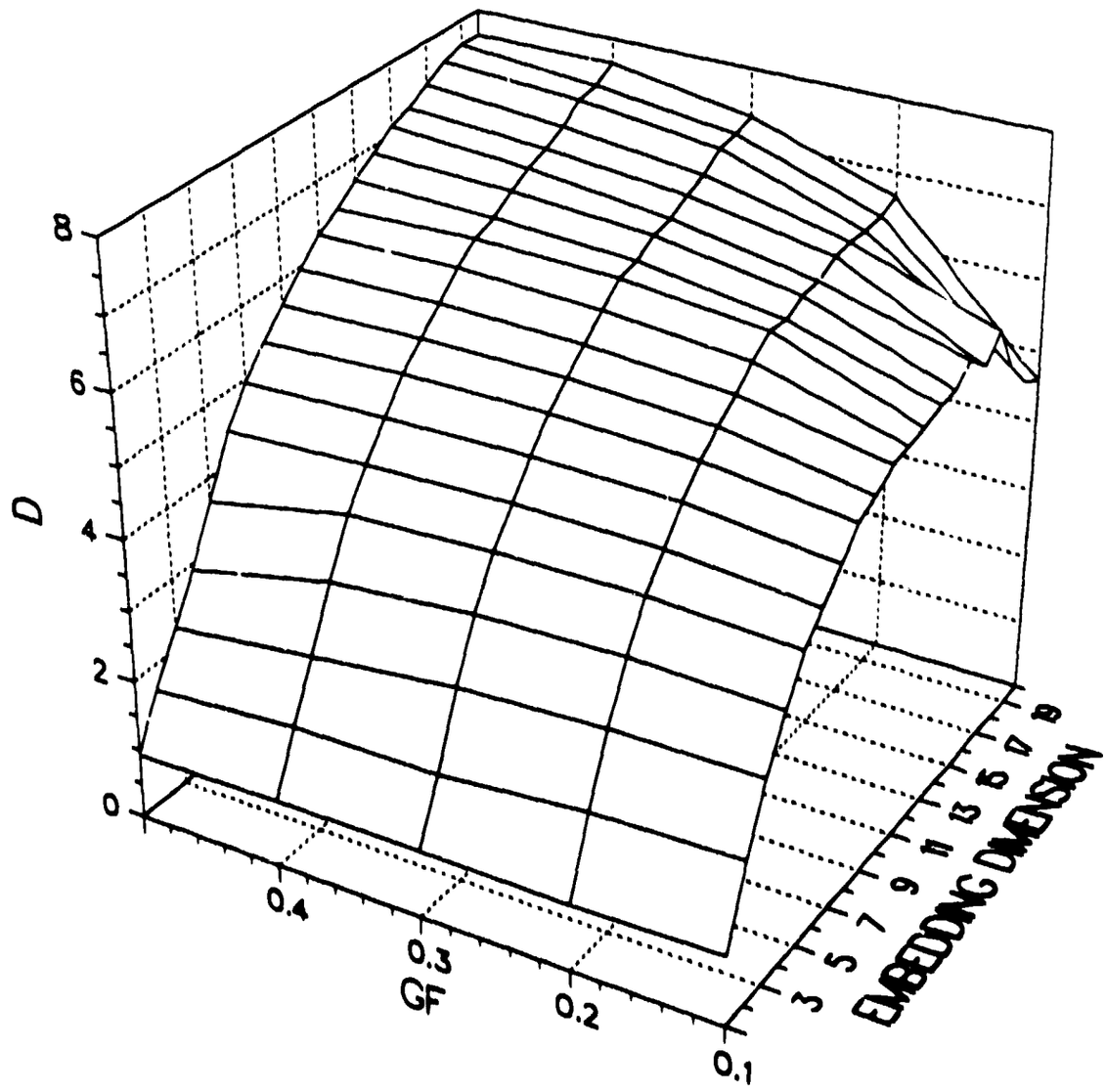

fig 15

2.FILE: 1SPH40

NSEG : 1 NDTOT : 15360 NDAT : 15142
NREF : 200 KREF : 100 FITGUE: 0.20
IRNU1 : 8 NDELAY: 11 NWIND : 4
NREFOK :83 DIM20: 6.66 STA20: 1.99
NO SING. VALUE DECOMPOSITION

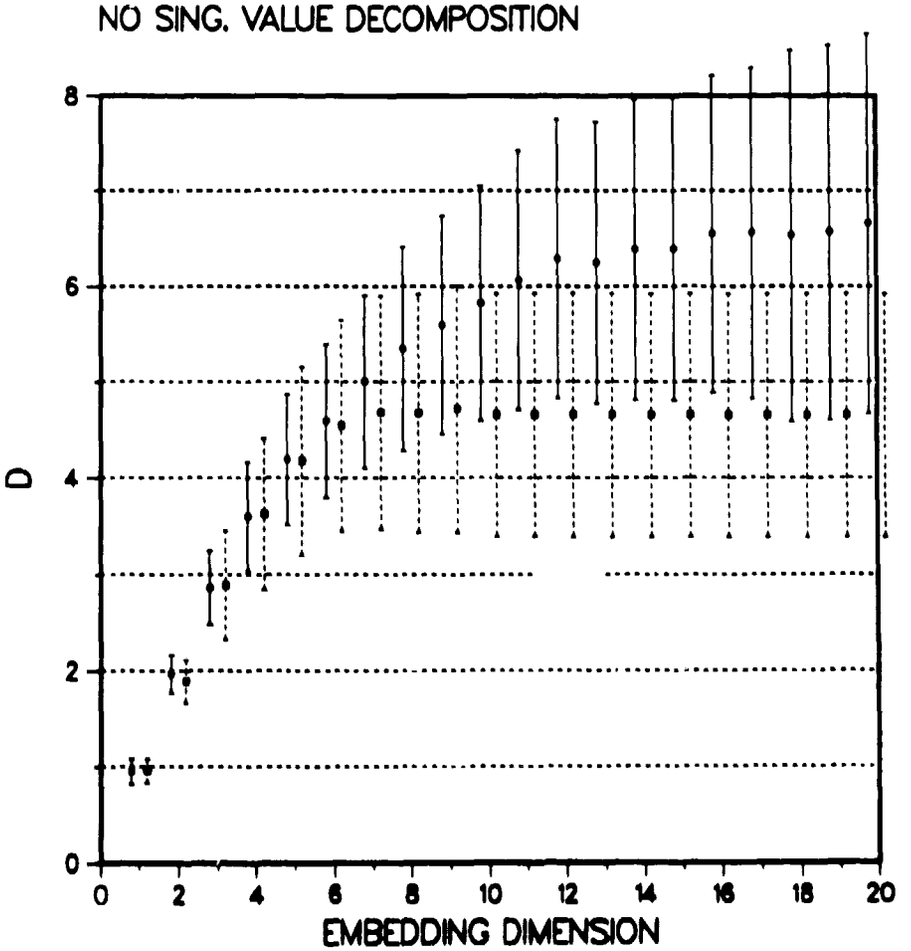

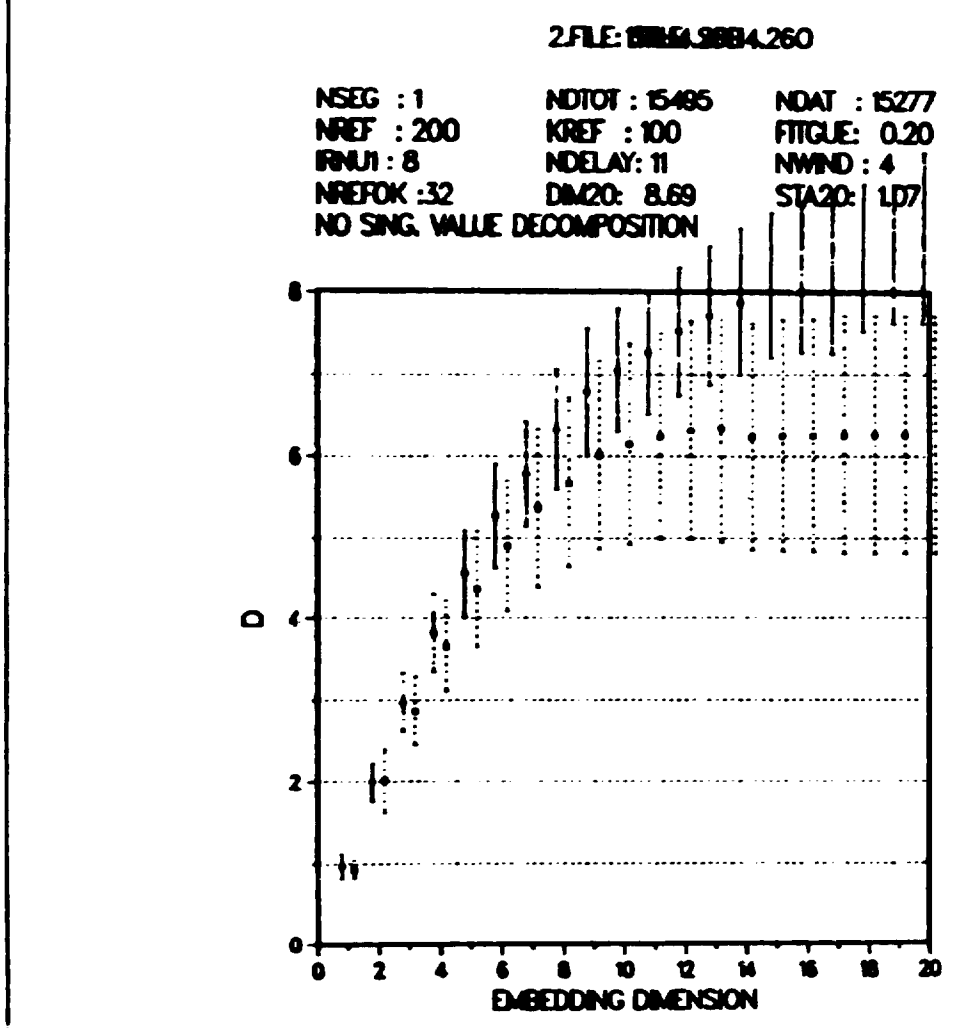
2.FILE: [redacted].260
NSEG : 1
NDTOT : 15495
NDAT : 15277
NREF : 200
KREF : 100
FITGUE: 0.20
IRNU1 : 8
NDELAY: 11
NWIND : 4
NREFOK :32
DM20: 8.69
STA20: 1.07
NO SING. VALUE DECOMPOSITION
D
EMBEDDING DIMENSION

1FILE: SPHERZ

NSEG : 2	NDTOT : 1580	NDAT : 1389
NREF : 200	KREF : 100	FITGUE: 0.20
IRNU1 : 4	NDELAY: 4	NWIND : 4
NREFOK :197	D0420: 4.84	STA20: 1.85

NO SING. VALUE DECOMPOSITION

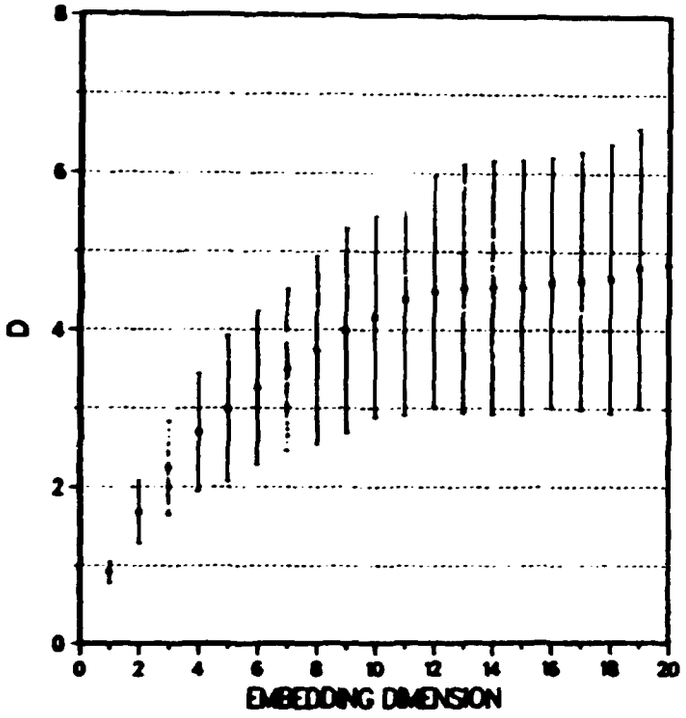

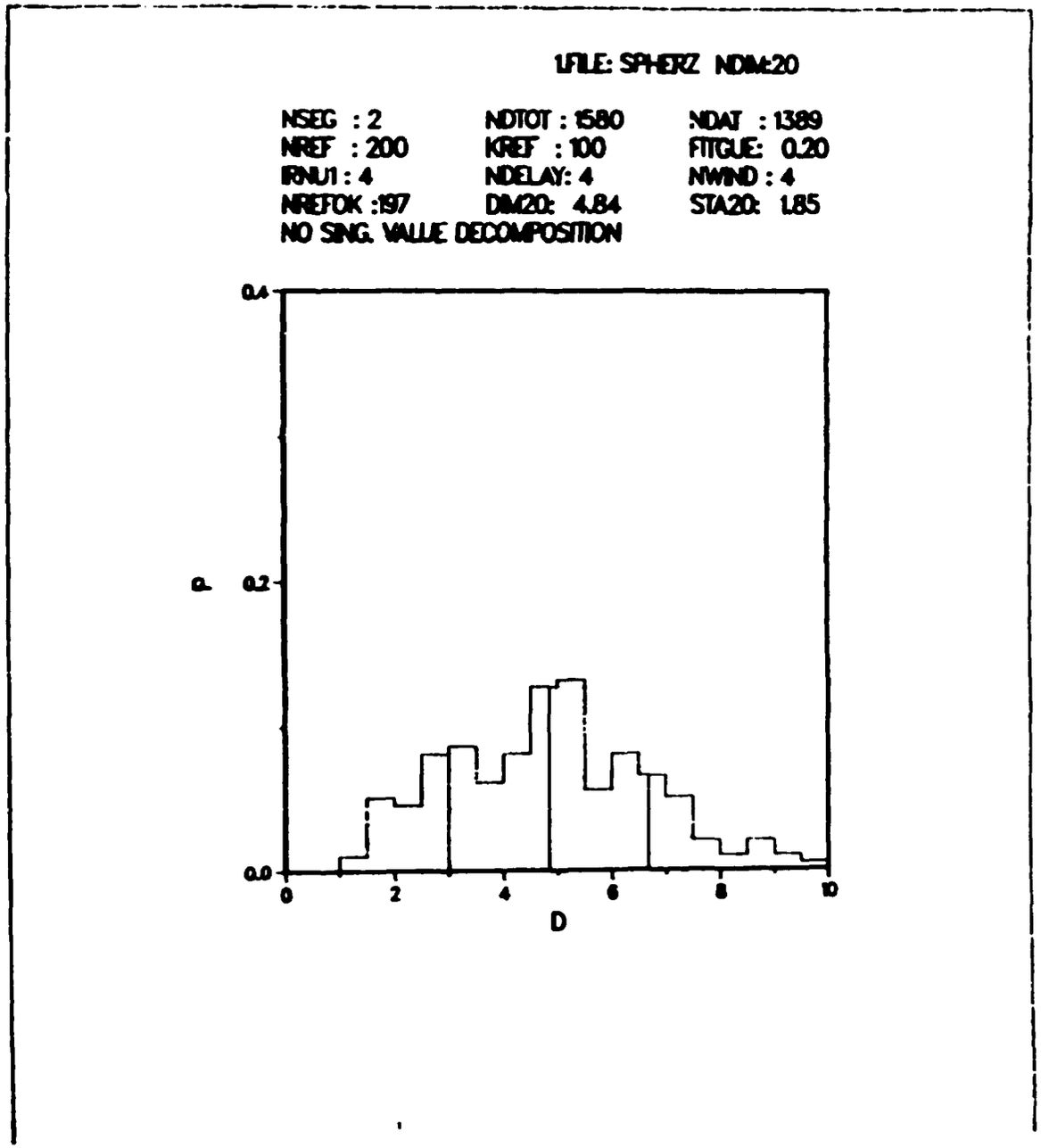
1FILE: SPHERZ NDIM:20
NSEG : 2
NDTOT : 1580
NDAT : 1389
NREF : 200
KREF : 100
FITGUE: 0.20
IRNU1 : 4
NDELAY: 4
NWIND : 4
NREFOK :197
DIM20: 4.84
STA20: 1.85
NO SING. VALUE DECOMPOSITION
0.4
0.2
0.0
P
0
2
4
6
8
10
D

1.c 13

GRASSBERGER
SLOPE 5.003, FIT : 0.034
SLOPE + 7.436 - 7.436
FILE NO.330, REF:200, DATA:100000
DELAY:11,EMB. DIM.:20

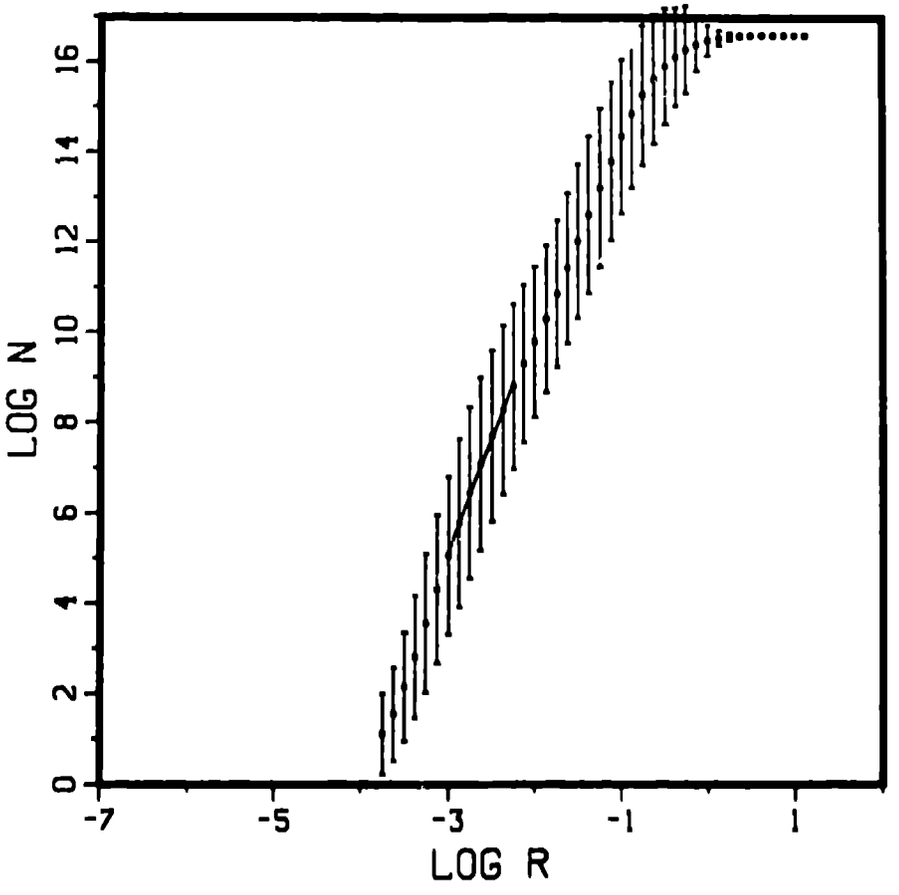

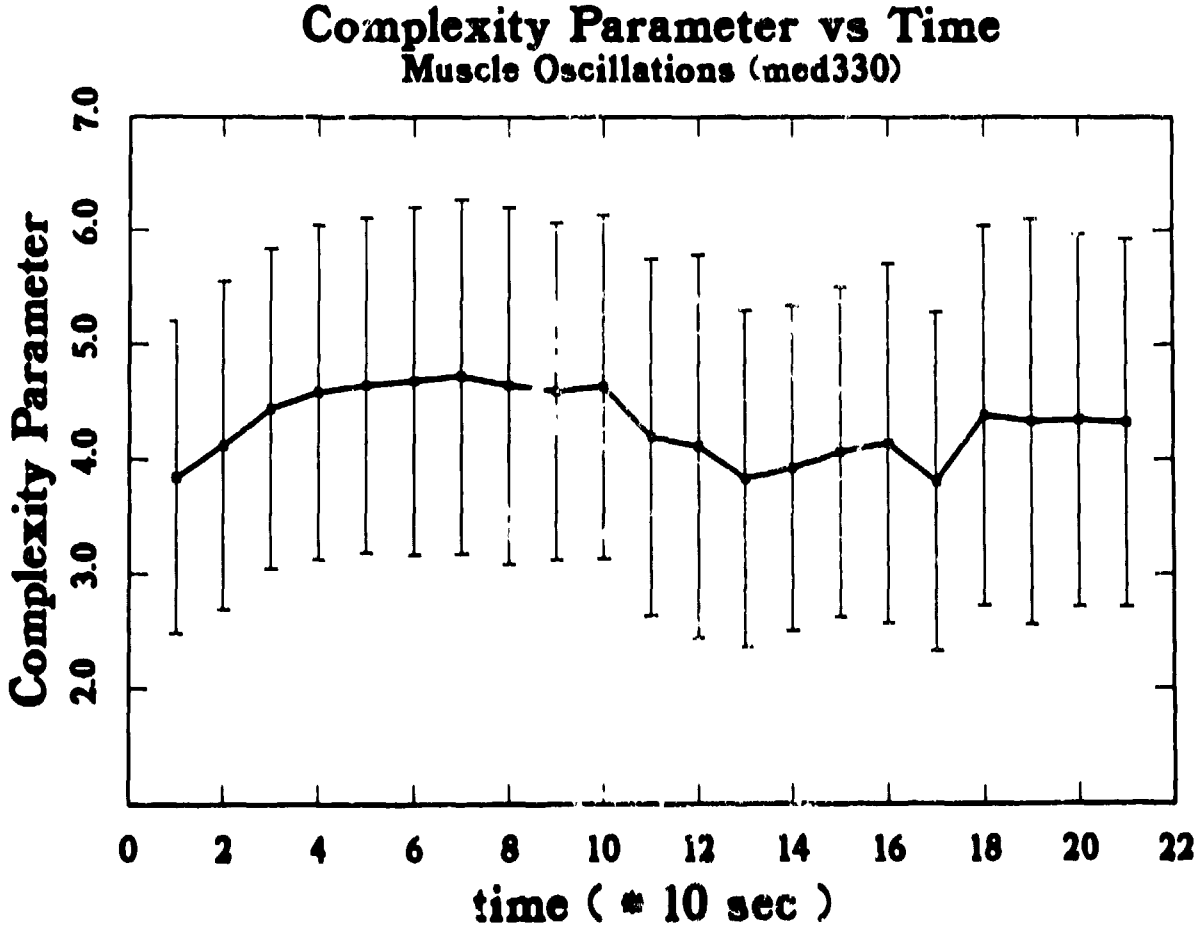
Complexity Parameter vs Time
Muscle Oscillations (med330)
Complexity Parameter
2.0
3.0
4.0
5.0
6.0
7.0
0
2
4
6
8
10
12
14
16
18
20
22
time (* 10 sec)

REF. PT.

D = 4.271 +/- 1.393 FIT 10.005
FILE NO.330, REF:200, DATA:100000
DELAY:11, DIMAX:20, POW:8

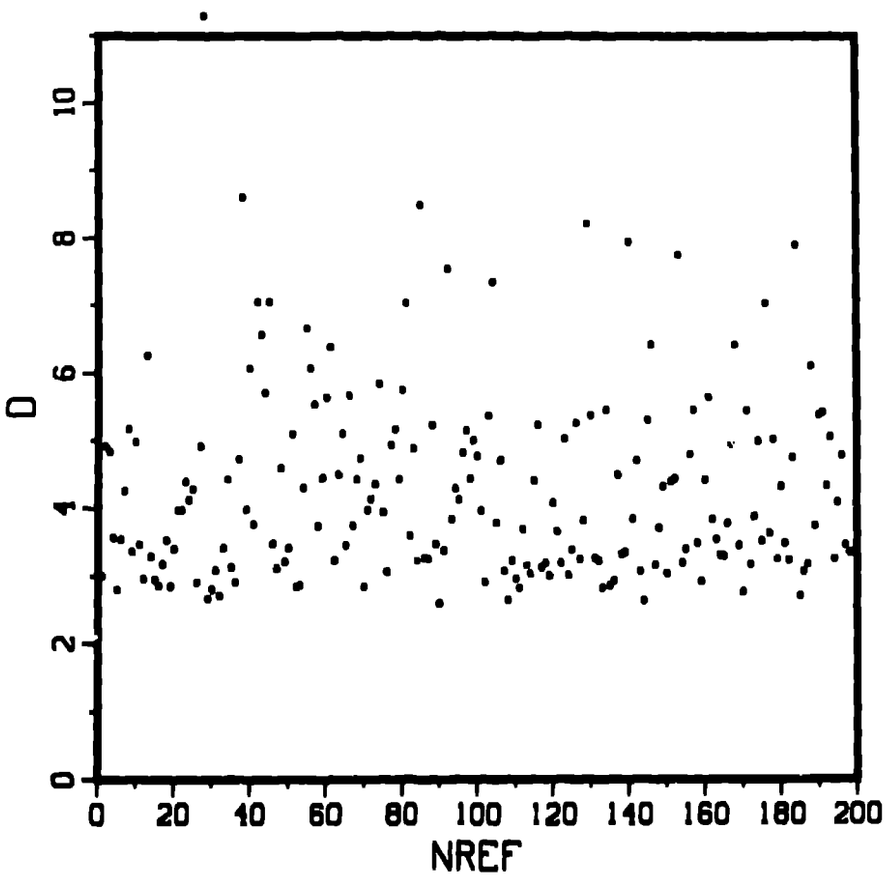

NDIM-20 #DIMS-200 D- 4.27 SD- 1.4 #BINS-20